ERDC/CRREL TR-00-14

Cold Regions Research
and Engineering Laboratory

US Army Corps
of Engineers®
Engineer Research and
Development Center

Cazenovia Creek Ice-Control Structure

James H. Lever, Gordon Gooch, and Steven Daly

August 2000

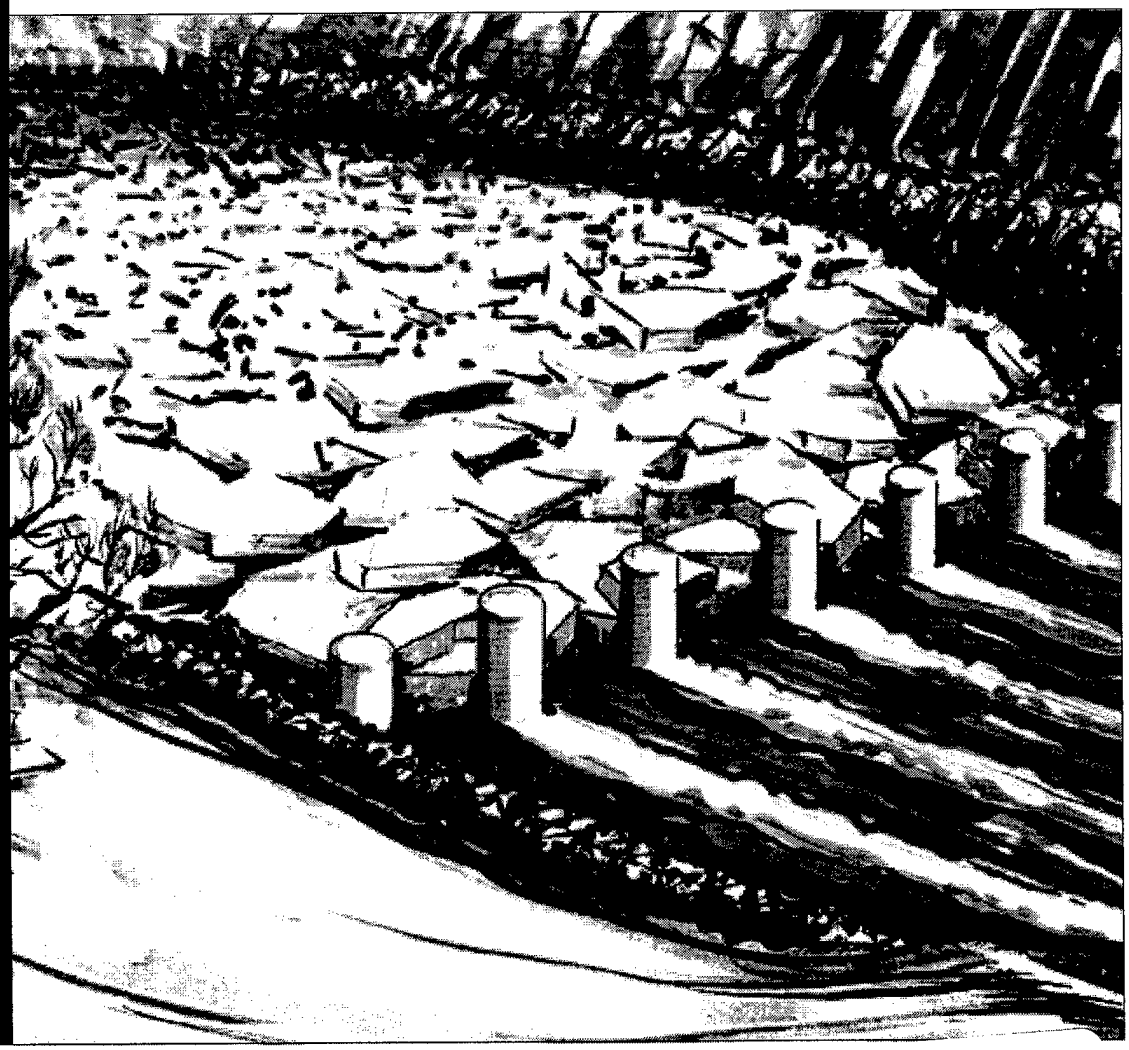

Technical Report
ERDC/CRREL TR-00-14

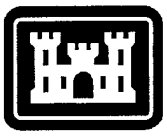

US Army Corps
of Engineers®
Cold Regions Research &
Engineering Laboratory

Cazenovia Creek Ice-Control Structure

James H. Lever, Gordon Gooch, and Steven Daly

August 2000

Prepared for
U.S. ARMY ENGINEER DISTRICT, BUFFALO

Abstract: Cazenovia Creek, in Western New York, is the largest tributary of the Buffalo River. Breakup ice jams form along the lower basin nearly every year during mid-winter or spring thaws, and ice-jam flooding occurs in the City of Buffalo and the Town of West Seneca about every 2–3 years. This report describes physical model tests and design recommendations for a new ice-control structure (ICS) for Cazenovia Creek. The recommended structure consists of nine 10-ft-tall × 5-ft-diameter cylindrical piers spaced across the main channel, and it uses the adjoining treed floodplain as a natural bypass channel. Also described are results from a numerical ice–hydraulic model to determine the extent of flooding induced upstream of the new ICS. Although few structures are affected, the ice jam held by the ICS will cause minor flooding of properties abutting the creek. However, the stream-wise extent of this flooding will decrease during an event as melting and washouts reduce the volume of ice in the jam. The structure balances the need to protect downstream areas from natural ice-jam flooding and the need to minimize upstream flooding induced by the retained ice.

How to get copies of CRREL technical publications:

Department of Defense personnel and contractors may order reports through the Defense Technical Information Center:

DTIC-BR SUITE 0944
8725 JOHN J KINGMAN RD
FT BELVOIR VA 22060-6218
Telephone (800) 225-3842
E-mail help@dtic.mil
msorders@dtic.mil
WWW http://www.dtic.mil/

All others may order reports through the National Technical Information Service:

NTIS
5285 PORT ROYAL RD
SPRINGFIELD VA 22161
Telephone (703) 487-4650
(703) 487-4639 (TDD for the hearing-impaired)
E-mail orders@ntis.fedworld.gov
WWW http://www.ntis.gov/index.html

A complete list of all CRREL technical publications is available from

USACRREL (CEERD-IM-HL)
72 LYME RD
HANOVER NH 03755-1290
Telephone (603) 646-4338
E-mail erhoff@crrel.usace.army.mil

For information on all aspects of the Cold Regions Research and Engineering Laboratory, visit our World Wide Web site:

http://www.crrel.usace.army.mil

PREFACE

This report was prepared by Dr. James H. Lever, Mechanical Engineer, Gordon Gooch, Civil Engineering Technician, and Dr. Steven F. Daly, Research Civil Engineer, of the Ice Engineering Research Division of the Cold Regions Research and Engineering Laboratory (CRREL) of the U.S. Army Engineer Research and Development Center (ERDC).

Funding for this work was provided by the U.S. Army Engineer District, Buffalo (CELRB), in partnership with the Town of West Seneca, New York, and the State of New York.

The authors gratefully acknowledge the assistance provided throughout this study by CELRB personnel, including Ed Gustek, Larry Sherman, and Phil Berkeley, and by Mike Kerl of the Town of West Seneca. They also thank Andrew Tuthill and Dr. J.-C. Tatinclaux for their suggestions to improve the manuscript. The authors also acknowledge the long-term research support by the Corps of Engineers' Cold Regions Research Program, without which low-cost ice-control structures for small rivers could not have been developed.

For the convenience of the sponsors, this report was prepared using customary U.S. units. A metric-conversion table is included.

CONTENTS

ILLUSTRATIONS

Figure

Figure

TABLES

Table

CONVERSION FACTORS: U.S. CUSTOMARY TO METRIC (SI) UNITS OF MEASUREMENT

These conversion factors include all the significant digits given in the conversion tables in the ASTM *Metric Practice Guide* (E 380), which has been approved for use by the Department of Defense. Converted values should be rounded to have the same precision as the original (see E 380).

Multiply	By	To obtain
inch	25.4	millimeter
foot	0.3048	meter
$foot^3$	0.02831865	$meter^3$
mile	1609.347	meter
$mile^2$	2,589,998	$meter^2$
$foot^3$/second (cfs)	0.0004719474	$meter^3$/second
foot-pound	1.335818	newton-meter
pound	4.448222	newton
pound/$inch^2$ (psi)	6894.757	pascal
Btu/lb_m	2326.000	joule/kilogram
Btu/lb_m °F	4186.800	joule/kilogram kelvin
Btu/ft^3 °F	67,066	joule/$meter^3$ kelvin
Btu/ft^3	37,259	joule/$meter^3$
degrees Fahrenheit	$t_C = (t_F - 32)/1.8$	degrees Celsius

Cazenovia Creek Ice-Control Structures

JAMES H. LEVER, GORDON GOOCH, AND STEVEN F. DALY

INTRODUCTION

Project Overview

Cazenovia Creek, located in western New York State, is the largest tributary of the Buffalo River (Fig. 1). Its basin is subject to heavy lake-effect snow from Lake Erie, and spring runoff typically has a strong snowmelt component. During most winters, ice covers 80–100% of the surface of the creek, and its average thickness ranges from 1 to 2 ft. Breakup ice jams form nearly every year during midwinter or spring thaws, and flooding occurs along the lower basin in the City of Buffalo and the Town of West Seneca about every 2–3 years. Some of these floods have caused damages exceeding $1,000,000, and one death has occurred.

During the 1980's, the U.S. Army Engineer District, Buffalo (CELRB), investigated the feasibility of building an ice-control structure (ICS) to reduce ice-jam flood damages along Cazenovia Creek in the Town of West Seneca (U.S. Army 1986a, 1986b). Based on model tests at CRREL (Gooch and Deck 1990), the ICS chosen consisted of a 6-ft-high × 250-ft-wide

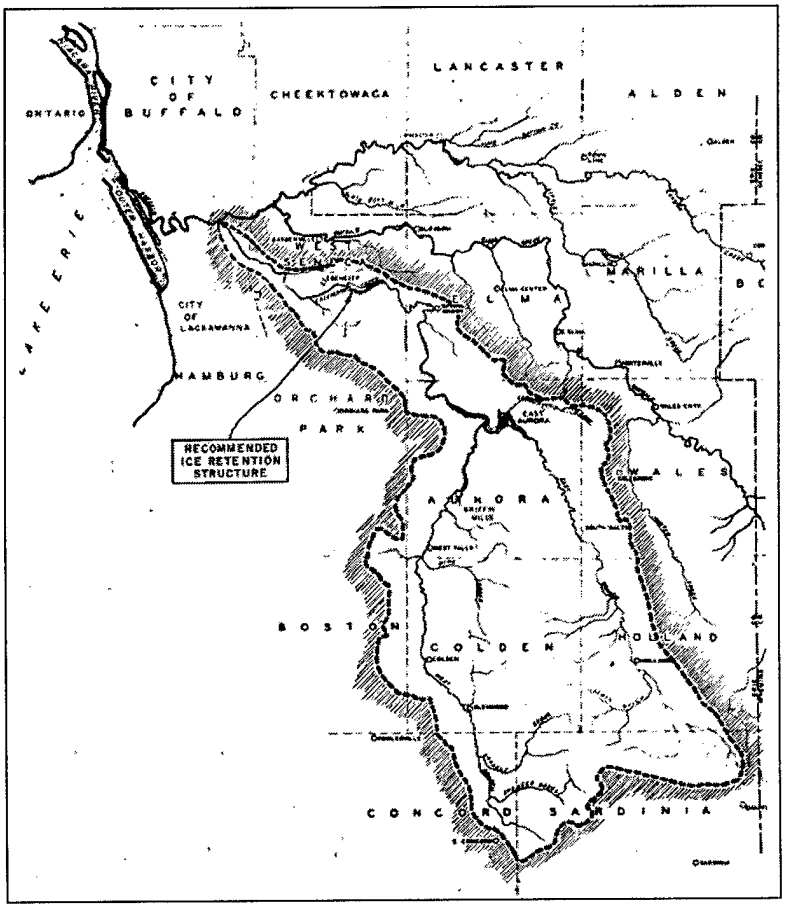

Figure 1. Cazenovia Creek drainage basin. (From USACE 1975.) The new cylindrical-pier ICS would be located at the same site originally proposed for a weir-with-piers ICS or "ice retention structure" (USACE 1986a, 1986b).

TO CONTENTS

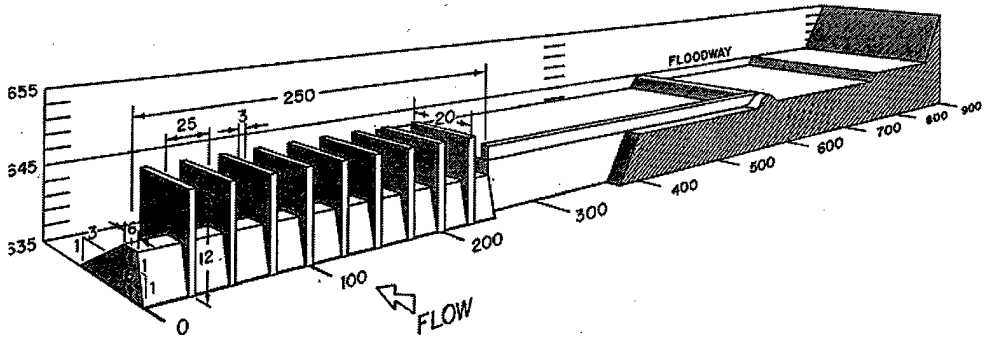

Figure 2. Concept drawing of original Cazenovia Creek ICS. Dimensions and elevations shown are prototype feet. Not shown is a low-flow gated opening in the weir to allow fish passage from spring to early winter. In its final design, the ICS piers were 12 ft long. A pool for storage of ice floes was to be excavated pool at elevation 635; it was 400 ft wide at the ICS and tapered linearly to the natural channel width (approximately 160 ft) at a distance of 600 ft upstream. The project also required extensive grading and riprap protection for the floodway bypass channel.

weir with nine ice-retaining piers, an excavated pool to store ice pieces, and a prepared floodway to bypass the peak flow (Fig. 2). The project was estimated to cost $2,100,000 (1987 dollars), reduce average annual ice-jam flood damages by $320,000 (1987 dollars), and achieve a benefit/cost ratio of about 1.5 over the life of the structure. Nevertheless, it was not built. Federal law was changed at that time to require 25% cost sharing by the local sponsor. The Town of West Seneca could not afford this amount on its own, and New York State had not yet modified its laws to participate as a sponsor.

Many communities along small northern rivers experience severe ice-jam flooding. Although flood damages can be significant, ICS's that include weirs, dams, or levees are often too expensive to achieve benefit/cost ratios over unity. In 1991, CRREL began research specifically to reduce ICS costs for small rivers. The result for breakup ice jams was the sloped-block ICS, developed using model tests, and demonstrated in the Lamoille River in Hardwick, Vermont (Lever et al. 1997, Lever and Gooch 1998). The Hardwick ICS consists of four massive, sloped blocks placed across the river adjacent to a treed floodplain. The blocks arrest a breakup ice run and form a stable, partially grounded ice jam. Trees on the floodplain retain ice pieces in the river channel while allowing flow to bypass the structure. The large gaps between blocks (14 ft) allow easy fish and canoe passage.

The sloped-block ICS has performed well, and no ice-jam flooding has occurred in Hardwick since its construction in 1994. However, for ice less than 1 ft thick, the ICS released the ice jams after several hours. This does not pose a problem in Hardwick and is a consequence of the safety-valve feature of the sloped blocks to minimize peak loads (and construction costs). But many areas downstream of the Cazenovia ICS site, in both West Seneca and Buffalo, are heavily developed. Consequently, we sought greater ice-retaining capacity for the Cazenovia ICS.

Figure 3 shows the new ICS concept proposed for Cazenovia Creek. It consists of evenly spaced cylindrical piers anchored in main channel and does not include a weir. The adjacent treed floodplain is left intact to act as a flow-bypass channel. In proposing this ICS, we expected that vertical piers spaced the same distance apart as the Hardwick ICS blocks would offer significantly better ice-retention capability, especially for thinner ice. Nevertheless, we needed to quantify this and verify that piers alone would offer the same or better performance as the original weir-with-piers ICS. Also, we needed to determine design ice loads on the piers. We therefore conducted physical model tests of the new ICS.

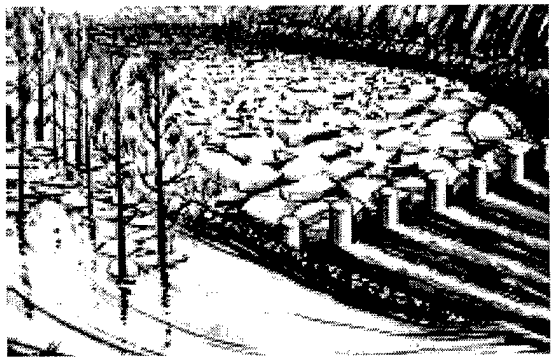

Figure 3. Concept drawing of new Cazenovia Creek ICS. Cylindrical piers of 5 ft diameter × 10 ft tall with 10- to 14-ft gaps anchored in main channel (no weir) arrest a breakup ice run and retain the ice jam throughout an event. Treed floodplain bypasses flood flow but not ice floes. Raised riprap embankment near ICS prevents scour and ensures floodplain flow returns to main channel downstream of ICS. The riverbed at the ICS site is bedrock.

These test results showed that, as expected, the cylindrical-pier ICS will retain an ice jam at discharges much higher than that needed to release a natural ice jam. Consequently, upstream water levels will increase compared to existing conditions. We used a numerical ice–hydraulic model to determine the maximum water surface elevations upstream of the structure and the location beyond which the ICS should cause no effect. CELRB then used these results to establish real estate requirements for project construction.

This report describes the model tests of the new Cazenovia Creek ICS, the design recommendations based on those tests, and the ICS's expected upstream effects. Where possible, we compare results with the original weir-with-piers ICS. Note that all physical units reported here are *prototype* scale, including those derived from model tests. All elevations quoted are National Geodetic Vertical Datum (NGVD).

Ice–hydraulic conditions

Figure 1 shows a map of the Cazenovia Creek watershed in western New York. The drainage area is 144 mi^2. The main stem of the Cazenovia Creek is about 17 miles long from the confluence of the creek's east and west branches in East Aurora to the Buffalo River. Its average slope along this section is 0.0026 or about 14 ft/mile.

As mentioned earlier, snowmelt and rainfall events in mid-winter and early spring have caused numerous ice-jam floods along Cazenovia Creek in West Seneca and Buffalo. The main stem contributes most of the ice volume to these jams. Increasing discharge fractures the ice cover, lifts it free of the banks, and sends it downstream as a surge of water and ice floes. Shear walls (i.e., walls of packed ice) have been observed from Transit Road to Mill Road, indicating at least temporary formation of ice jams. However, the damage-causing ice jams form when the ice run encounters the strong, thick ice sheet along the flatter reach below Mill Road. These jams may release after several hours and reform downstream until discharge is sufficient to clear ice into the Buffalo River and thence to Lake Erie.

About 134 mi^2 of drainage area lies upstream of the USGS Ebenezer gage at Ridge Road. Figure 4 shows stage hydrographs from the gage for ice jam floods occurring on 2 March 1972 and 23 February 1985. The hydrographs show characteristics typical of ice-jam events. The ice-affected stage increases slowly as the event begins. When an ice run passes the gage, the measured stage rises sharply and falls abruptly. The gage drops back to its open-water rating curve after the ice moves far downstream. The remainder of the hydrograph, including the broad peak, is unaffected by ice and can provide accurate discharge measurements. For

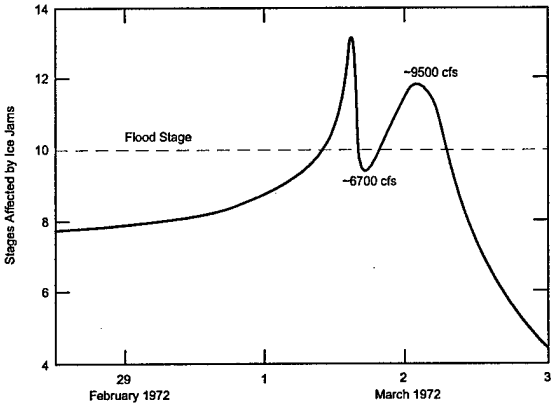

a. 2 March 1972. (After U.S. Army 1972.)

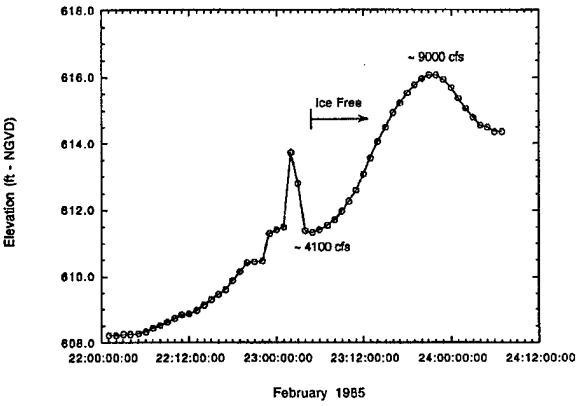

b. 23 February 1985

Figure 4. Hydrographs from USGS Ebenezer gage for two ice-jam events.

the 1972 and 1985 events, the discharges corresponding to the broad, open-water peaks were about 9500 and 9000 cfs, respectively. The maximum discharge of record (since 1941) was 13,500 cfs on 1 March 1955. The maximum discharge occurring during a known ice-jam event was 12,600 cfs on 22 January 1959. Ice thickness prior to breakup ranges widely, but few flooding problems have occurred for ice thinner than about 10 in.

The site selected for both ICS concepts lies about 2300 ft upstream of Mill Road (Fig. 5). The creek at this location drains 129 mi^2, its main channel is about 150 ft wide and 7 ft deep, and the undeveloped, treed floodplain is about 400 ft wide. The channel bed through the 2000-ft-long ICS reach consists of shale bedrock and has an average slope of 0.001; this slope increases to about 0.003 for the next 4 miles upstream. For 11 miles upstream of Mill Road, the creek flows through an incised valley that contains very little developed property.

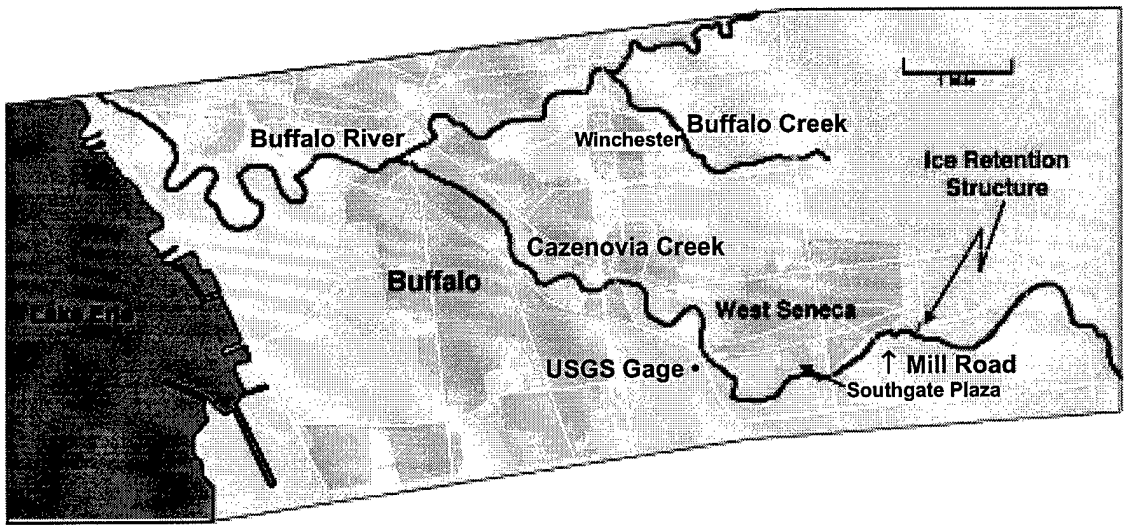

Figure 5. Lower basin of Cazenovia Creek and the site of the ice-control structures discussed here.

ICS DESIGN

Original ICS features and function

The original weir-with-piers ICS (see Fig. 2) was based on a similar structure installed on the Ste. Anne River in St. Raymond, Quebec (Deck 1984). In early winter, a low-flow opening would be closed to create a pool and form an ice sheet. The weir and excavated pool were sized to reduce water velocities sufficiently to store ice floes arriving from upstream during breakup. Piers protruded above the weir to stabilize the ice sheet and prevent passage of ice floes over the weir. A prepared floodway helped reduce velocities over the weir at high flows.

Gooch and Deck (1990) conducted physical model tests to optimize this ICS. They determined that ice breakup typically begins at about 1500 cfs and that the seven ice-jam floods on Cazenovia Creek from 1971–82 had peak discharges less than 6000 cfs. The Corps accepted this value as the design discharge for the original ICS (U.S. Army 1986a), although the hydrographs for the 1972 and 1985 events indicate that discharge can exceed this value during later stages of breakup events (see Fig. 4).

Gooch and Deck modeled about 4200 ft of river using scales of 1:40 horizontal and 1:10 vertical, and used urea-doped ice to scale ice flexural strength (prototype target 800 kPa or 120 psi). Test results indicated that a 6-ft-high weir with piers retained ice more effectively than an 8-ft-high weir with no piers (U.S. Army 1986a). For fewer than five piers, the ice sheet would extrude past the piers, or break up in front of them, and the ice floes accumulated in the pool would spill over the weir (Gooch and Deck 1990). Even with no floodway, the 6-ft-high weir with five or nine piers was found to retain ice to the design discharge (6000 cfs, which was also the maximum discharge possible in the model). Floodway flow reduced the flow over the weir by about 20% at the design discharge, providing some safety margin. For its final design, CELRB selected the 6-ft-high weir with nine piers and the prepared floodway, reasoning that increased reliability outweighed the small incremental cost (U.S. Army 1986a). Existing trees were to be left intact along the floodway to prevent ice passage downstream at high flows.

The weir-with-piers ICS would have required annual maintenance. All the estimated bed-load sediment and some of the suspended sediment were expected to deposit in the pool upstream of the ICS. Dredging of about 4000 ft^3 of sediment annually would have been needed to ensure adequate ice-storage volume (U.S. Army 1986a).

With the inclusion of a low-flow opening, no significant long-term environmental impacts on water quality or stream ecosystems were expected to result from the original ICS. Also, open-water flooding upstream was not expected to increase because increased water-surface elevations caused by the structure would extend no further than 4500 ft upstream (U.S. Army 1986a). Upstream effects with ice included were not examined, based on the assumption that all upstream ice would collect within the ICS pool.

Physical model of cylindrical-pier ICS

The main requirement for the new, cylindrical-pier ICS is to perform as well as the weir-with-pier ICS. That is, it should arrest breakup ice runs and retain the resulting ice jams (for ice thicker than about 0.8 ft) for the 6000-cfs design discharge (12-hour rise time). In

addition, any ice releases should be gradual, not catastrophic, and the ICS should have minimal environmental impact and low operation and maintenance requirements. The objectives of the model tests were to quantify the ice-retention capability of the new ICS, optimize pier spacing, and determine design ice loads.

We designed the physical model based on our experience with the sloped-block ICS (Lever et al. 1997). In particular, we selected a large scale-factor (1:15 undistorted) to study the unsteady ice-jam processes that occur near the ICS. For vertical piers, the gap between piers, rather than their diameter or shape, should have the strongest effect on the ICS's ice-retention capability. Therefore, we tested only 5-ft-diameter cylindrical piers and varied gap width from 10–14 ft. Tests of the sloped-block ICS indicated that they could retain ice jams that rose about 3 ft above the tops of the blocks. We therefore selected a single pier height, 10 ft above the average bed elevation at the ICS cross-section, which placed the top of the piers about 3 ft above the adjacent floodplain elevation. We also tested 8-ft-tall × 5-ft-wide, 45° sloped blocks to compare their performance with the cylindrical piers and to compare their model behavior with the field behavior of the Hardwick ICS.

Figure 6 shows a plan view of the 1:15-scale refrigerated hydraulic model of Cazenovia Creek used to develop the cylindrical-pier ICS. The model covered about 2000 ft of river length and 560 ft of width, and included most of the adjoining floodplain. The ICS was located in a channel section about 150 ft wide (Fig. 7). Time series measurements in the model included inflow, floodplain, and channel discharges, channel and floodplain water-surface elevations, and loads on five piers. Sample rate was 2.6 Hz (prototype scale). Single-axis load cells measured downstream overturning moments on four of the ICS piers (M1–M4), while a six-axis load cell measured downstream and transverse overturning moments and downstream force on one pier (Fig. 7). We calibrated the load cells before each test and zeroed

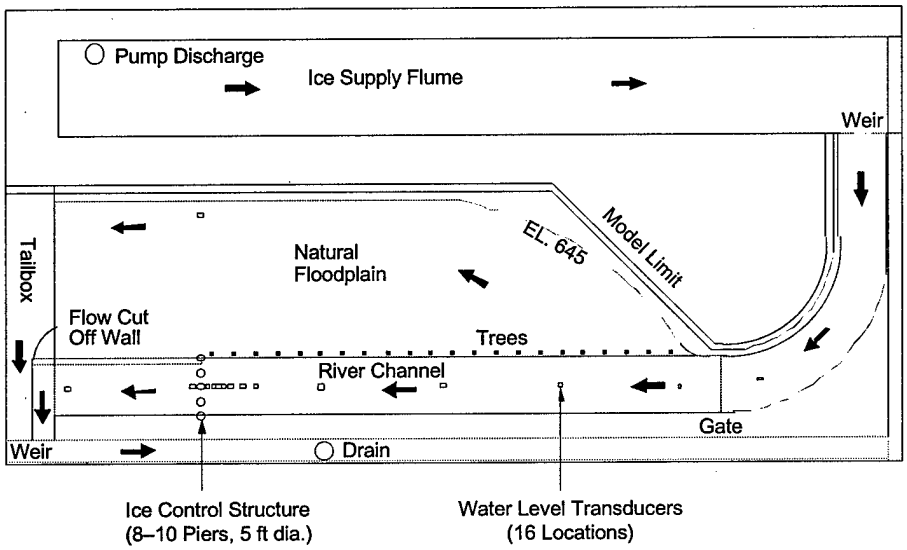

Figure 6. Plan view of 1:15-scale refrigerated hydraulic model of Cazenovia Creek. Channel width at the ICS is 150 ft, and the overall length modeled is about 2000 ft.

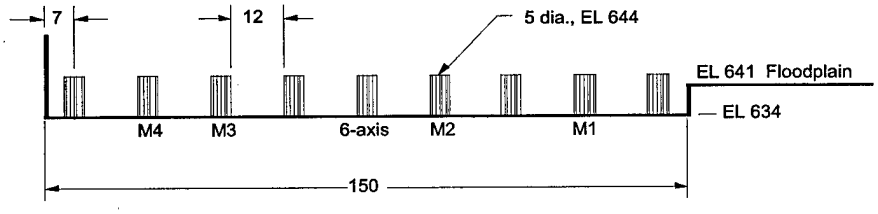

Figure 7. Elevation view of ICS consisting of nine 5-ft-diameter × 10-ft-tall cylindrical piers with 12-ft gaps. Dimensions and elevations (EL) are prototype feet. Piers M1–M4 were equipped with single-axis load cells to measure downstream overturning moments, and a six-axis load cell to measured downstream and transverse moments and downstream force.

Table 1. Froude scaling expressions between model (*m*) and prototype (*p*).

Parameter	*Scaling expression*
length	$L_p/L_m = 15$
velocity	$V_p/V_m = 15^{1/2}$
time	$T_p/T_m = 15^{1/2}$
discharge	$Q_p/Q_m = 15^{5/2}$
force	$F_p/F_m = 15^3$
moment	$M_p/M_m = 15^4$
ice strength	$\sigma_p/\sigma_m = 15$

them to remove the deadweight of the piers. Although they were fewer than the number of piers, we distributed these load cells to obtain representative results. We also manually measured ice thickness, flexural strength, and piece-size distribution, and video cameras recorded the tests. We used Froude scaling to relate model and prototype values (Table 1).

Most tests were conducted to simulate ice breakup along Cazenovia Creek. Ice covers about 1–2 ft thick were grown on the river channel and in the ice-supply flume. We would manually break the latter ice cover and feed it into the head of the model behind a porous gate. We would also partially break the ice cover in the river channel, usually leaving about 160 ft intact immediately upstream of the ICS. After establishing a base flow of 1000–1500 cfs, we would release the gate to simulate arrival of an ice run at the ICS reach. This ice run would form an ice jam, which would then collapse in stages onto the ICS as we increased discharge. The tests continued until the ice jam released or we reached maximum discharge (less than 8000 cfs) after about 10–12 hours (prototype). Figure 8 shows a typical ice jam formed by the cylindrical-pier ICS and the resulting floodplain flow.

Unless ice conditions are very mild (and thus pose little ice-jam threat), an ice sheet will be present upstream of the prototype ICS at breakup. Nevertheless, we conducted a few tests with no ice cover in the main channel upstream of the ICS because they represent a simpler case for validating a numerical model of breakup jamming at an ICS (Hopkins et al. 1996).

Model results

Table 2 summarizes the test conditions and results of the physical model study. We observed three main outcomes for tests with ice covers initially upstream of the ICS: 1) no release prior to the maximum pumping capacity, 2) slow washout of ice floes through a gap, and 3) rapid release of most of the jam through more than one gap. For discharges below 6000 cfs (the design discharge), there were no releases through the cylindrical-pier ICS, regardless of gap width. Releases took place above the design discharge on only three occasions (tests 18, 20, and 23), but in the only test where ice released over the cylindrical piers (test 18), the ice was relatively thin (0.89 ft) and the discharge had reached 9100 cfs. Washouts were more common and occurred for all three gaps tested, and it is difficult to discern a quantitative difference in performance. Qualitatively, however, the 14-ft-gap cylindrical-pier ICS tended to produce brief washouts at lower discharges and longer-duration washouts near maximum discharge, especially for thinner or weaker ice. We saw no qualitative or quantitative difference between the performance of the cylindrical-pier ICS for the two smaller gaps.

Comparable tests of the sloped-block and cylindrical-pier ICS's at the same pier gap (14 ft) illustrate the increased ice-retention capability of the latter structure. For moderate ice thickness (1.0–1.1 ft) and strength (70–100 psi), the ice jams washed out between or released over the sloped-blocks at discharges below the design value (tests 13 and 14) but were held well beyond the design discharge by the cylindrical piers (tests 4 and 6).

a. Looking across ICS towards model trees on floodplain.

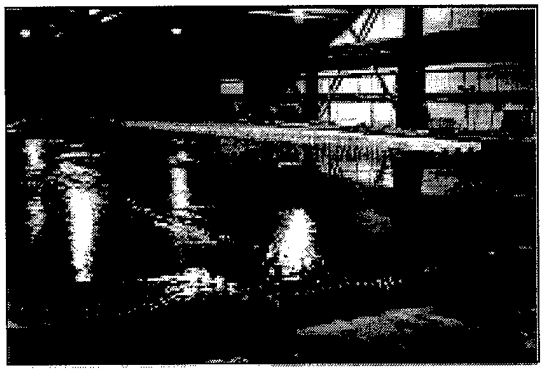

b. Looking upstream across floodplain.

Figure 8. Typical ice jam formed in model.

Table 2. Summary of test conditions and results obtained. ICS piers for tests 11–14 were 45° sloped blocks; D/S = downstream; all units prototype scale.

No.	Date	ICS gap (ft)	ICS diam. (ft)	Ice thick. (fr)	Ice flex. strength (psi)	Max. discharge (cfs)	Peak D/S moment, M_d (M ft-lb)	Peak D/S force, F_x (M lb)	D/S moment at F_x, M_d (M ft-lb)	Peak transv. moment, M_x (m ft-lb)	D/S moment at M_x, M_y (m ft-lb)	Result
1	11/17/98	14	5	1.7	61	2900	1.8	no data		no data		No release.
2	11/19/98	14	5	1.8	large floes	5000	0.92	0.10	0.92	0.31	0.92	No release.
3	11/25/98	14	5	1.0	no sheet	2900	0.24	0.020	0.10	0.0100	0.10	No jam (no sheet).
4	12/01/98	14	5	1.0	100	7000	1.0	0.097	0.68	0.14	0.36	Washout.
5	12/03/98	14	5	1.7	87	8100	1.3	0.096	0.71	0.12	0.58	No release.
6	12/15/98	14	5	1.1	75	8100	0.76	0.050	0.35	0.078	0.18	Washout.
7	12/17/98	14	5	1.7	170	8500	0.69	0.065	0.53	0.23	0.53	No release.
8	12/22/98	14	5	1.2	29	4700	0.98	0.13	0.98	0.20	0.98	Fracture & washout (weak ice).
9	12/24/98	14	5	1.5	no sheet	2900	no data	no data		no data		Release (no sheet).
10	12/31/98	14	5	2.2	no sheet	2900	0.43	0.031	0.22	0.17	0.20	Release (no sheet).
11	1/6/99	14	8x5-45°	1.8	140	8400	1.6	0.074	0.64	0.12	0.66	No release.
12	1/8/99	14	8x5-45°	1.5	72	9000	1.3	0.077	0.85	0.092	0.85	No release.
13	1/12/99	14	8x5-45°	1.1	74	5300	0.82	0.072	0.53	0.11	0.20	Release through middle gaps.
14	1/14/99	14	8x5-45°	1.1	72	5500	0.75	0.076	0.65	0.054	0.60	Washout.
15	1/20/99	10	5	1.1	81	5800	0.63	0.065	0.43	0.15	0.27	Washout (thin, 6-in. ice from white tank).
16	1/22/99	10	5	1.1	250	10000	0.53	0.083	0.48	0.086	0.33	No release (strong ice).
17	1/26/99	10	5	0.75	280	9000	0.98	0.12	0.98	0.10	0.15	Slow washout of smaller floes.
18	1/29/99	10	5	0.89	86	9100	0.82	0.065	0.45	0.20	0.35	Release (floe breakage & overtopping of piers).
19	2/1/99	10	5	1.5	110	11000	1.0	0.033	0.22	0.10	0.18	No release.
20	2/5/99	12	5	0.99	84	9200	0.76	0.076	0.48	0.16	0.33	Washout then release.
21	2/9/99	12	5	1.0	380	8600	1.3	0.042	0.21	0.11	0.21	No release (strong ice).
22	2/12/99	12	5	0.99	87	8200	0.93	0.10	0.59	0.14	0.22	No release.
23	2/17/99	12	5	0.97	64	7000	0.46	0.063	0.44	0.15	0.43	Washout then release.

TO CONTENTS

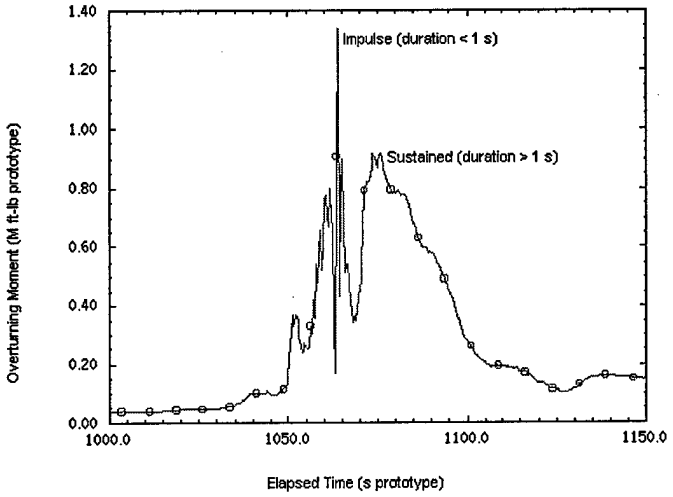

Figure 9. Measured downstream overturning moment (test 5, M1), showing peak impulsive and sustained moments.

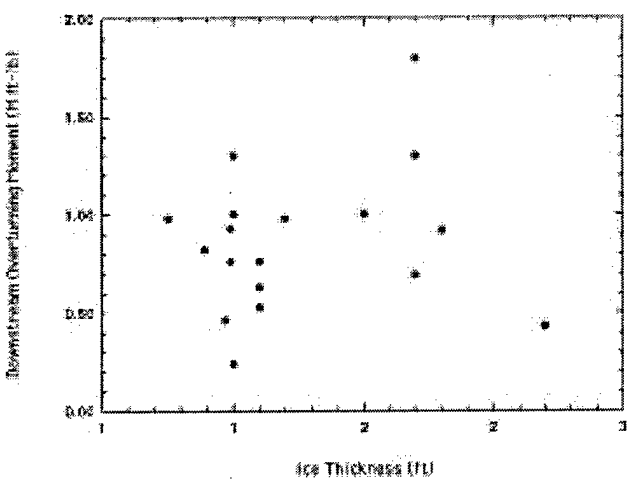

a. Versus ice thickness.

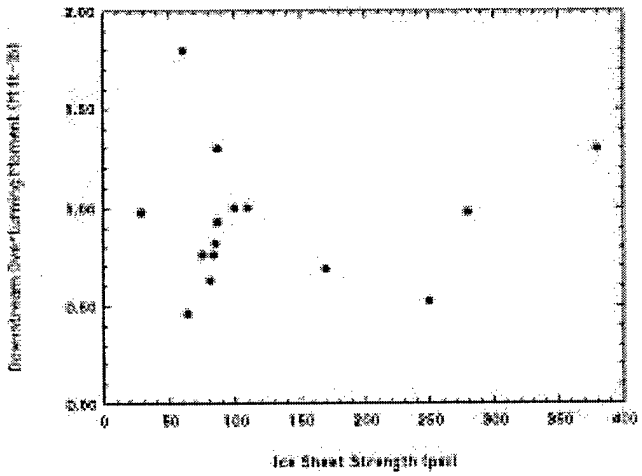

b. Versus ice flexural strength.

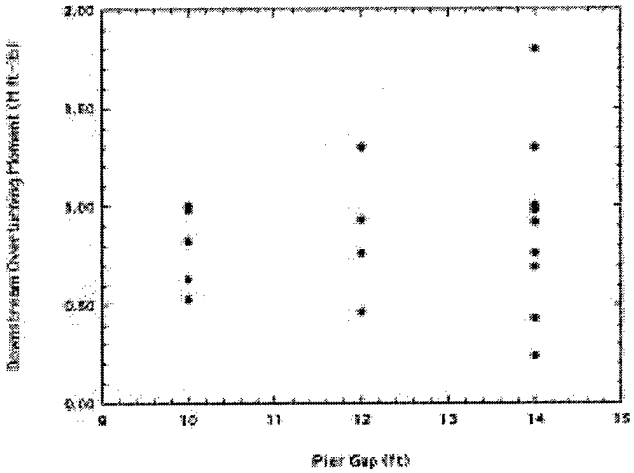

c. Versus gap between piers.

Figure 10. Scatter plots of peak overturning moments. The measured moments are essentially independent of these parameters within the ranges tested.

Figure 9 shows a time series record of the downstream overturning moment measured on a pier during ice-jam formation. Peak impulsive moments (duration less than 1 second) were usually caused by impacts of individual ice floes, while peak sustained loads developed during unsteady ice-jam formation and collapse events (which occurred on the order of 10–100 seconds). Montgomery et al. (1980) and Montgomery and Lipsett (1980) provide convincing evidence that even massive bridge piers can respond to impulsive loads caused by ice impacts. The natural frequency of a pier (typically 1–20 Hz) governs its response to these dynamic loads (Montgomery et al. 1980). Because the ICS piers will carry no superstructure, they should have frequencies at least as high as bridge piers, and even ice-impact loads will effec-

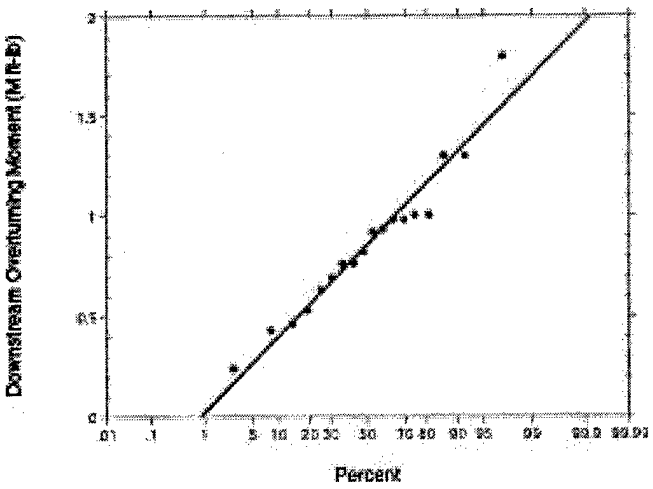

Figure 11. Cumulative probability for measured peak downstream overturning moments, M_d. The straight line represents the best-fit normal distribution to the data.

tively be long in duration. Thus, we selected the largest downstream moment, impact or sustained, measured on any of the five instrumented piers as the peak downstream moment for each test, M_d.

Table 2 shows the resulting values of M_d. Interestingly, these peak moments are not correlated with ice thickness, ice strength, or pier gap (Fig. 10). We also saw no dependence on pier location. This allows us to treat the M_d values as a single population and thereby develop a statistical basis for design loads. Figure 11 shows the resulting probability distribution for M_d plotted on a normal-probability scale. A straight line fits the data reasonably well, implying a normal distribution.

We also compiled for each test the peak downstream force, F_x, peak transverse overturning moment, M_x, and the downstream overturning moments at the times of those peaks, M_y, all measured by the six-axis load cell. As with M_d, F_x and M_x are not correlated with ice thickness, ice strength, or pier gap. From the ratio M_y/F_x, we may compute the effective moment arm, L_p, relating the measured downstream force to the downstream overturning moment (Fig. 12). This calculation assumes that vertical ice forces contribute negligibly to M_y, a reasonable assumption for cylindrical piers during breakup. Figure 13 shows that L_p tends to increase slightly for increasing M_y, indicating that rising ice-contact height and increasing downstream force both contribute to large downstream overturning moments. Similarly, Figure 14 shows that the ratio M_x/M_y tends to decrease for increasing M_y, although the correlation is not strong.

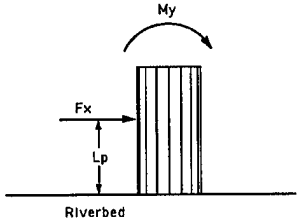

Figure 12. Effective moment arm, L_p, relating downstream ice force, F_x, to downstream overturning moment, M_y, measured on six-axis load cell.

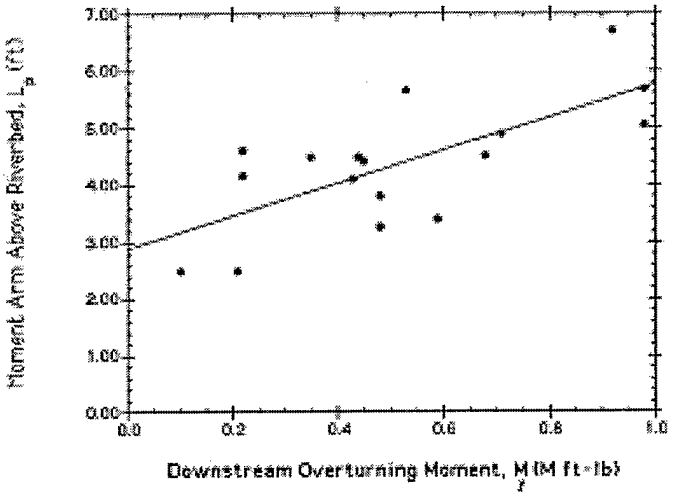

Figure 13. Effective moment arm, L_p, versus downstream moment, M_y, at the time of the peak downstream force, F_x, during each test.

In only one case (test 3) did the ICS not arrest the initial breakup ice run. This test began with no ice in the main channel upstream of the ICS. The test outcome agrees with observations at the Hardwick sloped-block ICS: after release of an initial jam, a subsequent ice run consisting of 1-ft-thick floes (or less) will not jam across the 14-ft gaps at the ICS. We repeated this test with thicker ice (tests 9 and 10) and found that the

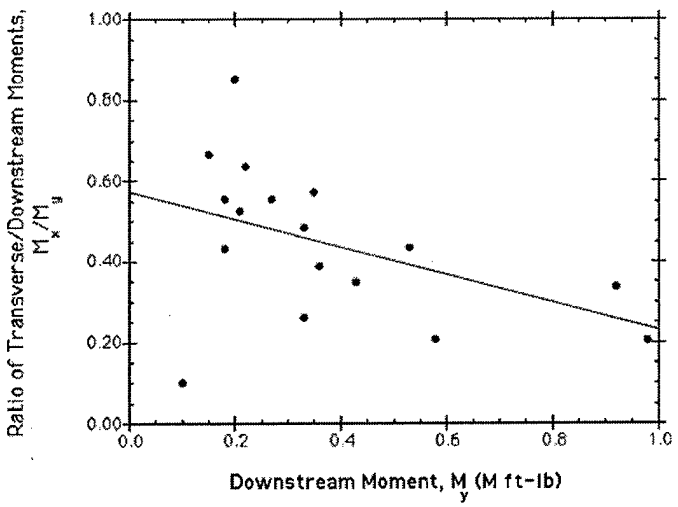

Figure 14. Ratio of transverse-to-downstream moments versus downstream moment, M_y, at the time of peak transverse moment, M_x, during each test.

cylindrical-pier ICS arrested the initial runs but released the resulting ice jams at about 50% of the design discharge. However, this scenario should not occur at the prototype ICS. The piers will form a small pool that will preferentially freeze early and solidly. With this ice upstream, the ICS will arrest an ice run and hold a jam well beyond the design discharge. Any later ice runs will impact and add to the jam rather than interacting directly with the piers.

Design ice loads

The model data can provide design ice loads for downstream and transverse overturning moments and forces. The peak downstream moments measured during each test were cast in a statistical framework for the purpose of determining these design loads. We recommend designing for loads at a cumulative-probability level of 99.9% and describe design loads here based on that probability. This corresponds to an average return interval of 1000 years, assuming one ice-breakup event per year. Design loads based on higher or lower probabilities can be determined using the same procedure.

The results on Figure 11 directly yield $M_d = 2.0 \times 10^6$ ft-lb as the design value for downstream overturning moment. We may use this value to estimate the other design loads. Because L_p tends to increase slightly for increasing M_y, we may obtain a conservative estimate of design value of the downstream force, $F_x = M_d/L_p$, by using the average value of $L_p = 4.4$ ft. This yields $F_x = 0.45 \times 10^6$ lb as the design value for downstream force. Similarly, because M_x/M_y tends to decrease for increasing M_y, we may obtain a conservative estimate of design value of the transverse moment, $M_x = (M_x/M_y) \cdot M_d$, by using the average value of $M_x/M_y = 0.45$. This yields $M_x = 0.90 \times 10^6$ ft-lb as the design value for transverse moment. Roughly speaking, the design downstream force acts halfway up the pier, and the design transverse moment is half of the design downstream moment.

These design loads may occur simultaneously on a pier because they often derive from the same event. For this reason, although we did not record transverse forces, F_y, we may estimate the design value as $F_y = M_x/L_p = 0.20 \times 10^6$ lb. This assumes that transverse and downstream moments act at the same height on the pier (4.4 ft above the bed) for the design event.

We may compare these results with the downstream loads used to design the original weir-with-piers ICS. Recall that its function was different. During breakup, floes arriving from upstream would collect in the pool upstream of the ICS, causing the overlying ice sheet to ride up the piers, essentially to their tops. The design value of the downstream ice load was assumed to result from the crushing failure of a 1-ft-thick sheet across the 3-ft width of the pier at a pressure of 262 psi, resulting in $F_x = 0.11 \times 10^6$ lb (U.S. Army 1986b). Although this is lower than F_x determined here, it acted much higher on the pier so that the design overturning moment was similar, $M_d = 1.5 \times 10^6$ ft-lb. Rather than experiencing ice-crushing failure, however, the piers in the present ICS are subjected to direct ice-floe impacts and unsteady ice-jam formation and collapse events.

It is also interesting to compare the recommended design loads with those resulting from application of the AASHTO (1998) design standards for bridge piers. These standards rely heavily on the work of Montgomery et al. (1984), which also formed the basis for design standards in Canada (CSA 1988).

The AASHTO standards differentiate among crushing (across the full width of a pier), bending, and impact ice-failure modes. They note that impact failure, where a small floe comes to rest before it has crushed

over the full width of the pier, can be the controlling mode on small streams (less than 300 ft wide). This mode provides the closest analogy to the ice-arrest function of the proposed ICS. For vertical piers, the applicable equation is (AASHTO 1998)

$$F_i = C_a \cdot p \cdot t \cdot w \cdot K_i \quad (1)$$

where

$$C_a = (5t/w + 1)^{0.5} \quad (2)$$

and p = effective crushing strength
t = ice thickness
w = pier width
K_i = impact reduction factor.

Here, $w = 5.0$ ft, and we may assume $t = 2.0$ ft for design purposes. Equation 2 then yields $C_a = 1.7$. The largest value of p suggested in the standard is about 220 psi, recommended for cases where breakup can occur when the average ice temperature is measurably below the melting point (e.g., mid-winter breakup). Lastly, K_i depends on A/r^2, where A is the floe plan area and r is the radius of the pier nose. The model tests suggest that floes larger than about 30 ft across seldom strike a pier at high velocity. For this case, $K_i \sim 0.7$ applies. These values combine, via eq 1, to predict $F_i = 0.4 \times 10^6$ lb, remarkably close to the design value suggested here.

The AASHTO standards do not provide quantitative guidance on the elevation at which to apply the ice-impact force to the pier, especially as these standards are not intended for the design of ice-control structures. For this purpose, the model tests probably provide the best guidance, $L_p = 4.4$ ft. Also, because they apply to bridge piers, the standards recommend simultaneous application of the downstream force and a transverse force equal to only 15% of that value. The simultaneous transverse force recommended here, based on model data, is 45% of the downstream force and is conservative compared to the standards.

Additional ICS features

The cylindrical-pier ICS uses the adjacent treed floodplain, located along the right bank of Cazenovia Creek (see Fig. 6), as a flow-bypass channel. This presents additional design requirements: preventing sediment scour along the right bank, preventing floodplain flow from reentering the main channel upstream of the ICS, and retaining the ice pieces in the main channel as flow diverts onto the floodplain. We may satisfy these requirements with additional ICS features.

Right-bank riprap

Model tests of the cylindrical-pier ICS and the sloped-block ICS (Lever et al. 1997) revealed that floodplain flow could reenter the main channel just upstream of the ICS, where water levels are below bank-full. This flow can erode the ice floes arched between the floodplain and the nearest structural element, causing early release of the ice jam. Furthermore, this flow is sufficiently fast to scour natural bank materials, threatening catastrophic release of the jam.

Riprap placed along the right bank near the ICS can prevent both problems. The riprap should extend at least one river width (about 150 ft) upstream and downstream of the ICS and be tied-off to existing ground. To control reentering flow, the top of the riprap should be about 2 ft above the local floodplain elevation, making it EL 643 here. A similar riprap emplacement at the Hardwick ICS has worked well to prevent scour and reentering floodplain flow.

Although dynamic ice-jam surges can occur near the ICS, the banks do not experience persistent ice action. Consequently, local flow velocities rather than ice action should govern the riprap design. At Hardwick, the riprap consists of granite stone with $D_{50} = 1.7$ ft, and it has shown no signs of failure. For the Cazenovia Creek ICS, $D_{50} = 2.0$ ft should be adequate.

Ice-retaining posts

The treed floodplain adjacent to the ICS allows flow to bypass the structure but retains ice in the main channel. However, several gaps exists in the trees along the right bank at the Cazenovia Creek ICS site. In these gaps, wooden posts should be installed to retain ice pieces in the main channel.

Posts installed in the physical model (see Fig. 6) retained most ice floes in the main channel during simulated breakup events. Maximum ice elevations along this right-bank "tree line" were 5–7 ft above the local floodplain elevation. We did not, however, measure loads on the posts. Much of the ice was grounded along the bank, and the water level drop across the posts was much less than 5 ft.

Wooden posts placed 6 ft on-center along the gaps in the right-bank trees are adequate to retain ice. The posts should protrude 4 ft above the top of the bank. We may conservatively assume that a 5-ft hydrostatic head acts across each post and that the resulting force acts 2 ft above the ground. Thus, each post must resist 12,000 ft-lb of overturning moment.

Dry, select-grade Douglas Fir and Southern Pine (long leaf) have allowable tensile stresses for static loads of about 1800 psi (CRC 1970). Thus, 10-in.-diameter posts of these woods are adequate to resist the estimated overturning moment; use of 12-in.-diameter posts is conservative. Note that allowable stresses may be increased by 100% for impact loads (CRC 1970), which should accommodate moments from ice impacts.

ICS design recommendations

We recommend an ICS consisting of nine 5-ft-diameter × 10-ft-tall cylindrical piers spaced with 12-ft gaps to reduce ice-jam flood damages along Cazenovia Creek. The ICS should be located at the same cross section as the original weir-with-pier ICS, and the top of the cylindrical piers should be at EL 644 ft.

The design ice loads on each pier (at a cumulative-probability level of 99.9%) can act simultaneously and are as follows:

$M_d = 2.0 \times 10^6$ ft-lb (downstream overturning moment)

$F_x = 0.45 \times 10^6$ lb (downstream force)

$M_x = 0.90 \times 10^6$ ft-lb (transverse overturning moment)

$F_y = 0.20 \times 10^6$ lb (transverse force).

Riprap, consisting of stone with D_{50} of about 2.0 ft, should be installed along the right bank at least 150 ft upstream and downstream of the ICS to prevent scour and ice erosion. The top of the riprap should be at EL 643 ft.

Dry, select-grade 12-in.-diameter wooden posts should be installed 6-ft on-center along the gaps in the trees along the right bank near the ICS. These posts should protrude 4 ft above the local top-of-bank elevations. Insofar as possible, existing trees on the floodplain should not be disturbed during construction.

UPSTREAM EFFECTS

Upstream issues

The cylindrical-pier ICS will arrest ice arriving from several miles upstream. It will retain the resulting ice jam at discharges much higher than the maximum discharge at which an ice jam would remain in the natural channel. While this should significantly reduce ice-jam flood damages downstream, water levels during ice events will be higher upstream of the ICS than under existing conditions. The project could thus affect upstream property owners.

Cazenovia Creek flows through a steep-walled valley from East Aurora to Mill Road. There are few structures located within this valley that are vulnerable to flooding. Table 3 lists such structures from the ICS to Transit Road, the upstream limit of this analysis. Figure 15 shows the topography of this reach. Most properties that abut the creek do not have structures within the valley.

The objectives here are to determine the maximum water level caused by the ICS for all locations upstream and to determine the location beyond which the ICS essentially has "no effect." We have taken this latter condition to be the location where the maximum water level induced by the ICS is below the 100-year open-water elevation under existing conditions. The information sought here is needed to determine the real estate requirements (e.g., flow easements, buy-outs, flood protection) to construct the ICS. We used a numerical ice–hydraulic model, with input from the physical model, to determine upstream effects of the ICS.

Ice breakup with ice-control structure

The physical model tests indicated that the ICS will arrest a breakup ice run and retain the resulting ice jam to discharges exceeding 6000 cfs without catastrophic ice releases (see Table 2). For the recommended ICS (12-ft-gaps), 1-ft-thick ice of moderate strength should start to wash out through the gaps at 7000–8000 cfs. The ICS should retain stronger or thicker ice to higher discharges. For example, the 12-ft-gap ICS held 1.0-ft-thick strong ice to 8600 cfs, even after we manually released ice at one of the gaps (test 21). Also, the 10-ft-gap ICS held 1.1-ft-thick strong ice and 1.5-ft-thick moderate-strength ice to 10,000 and 11,000 cfs, respectively, without major releases (tests 16 and 19). Smaller floes did wash out slowly (through the ICS gaps and onto the floodplain) during all tests, reducing the ice

Table 3. Structures within the Cazenovia Creek valley from the ICS site to Transit Road. Most properties that abut the creek do not have structures within the valley.

Name	*Description*	*Distance upstream of ICS (miles)*	*Flood elevation (ft-NGVD)*
Kotecki Grove	Commercial, picnic areas	0.27–0.36	648–650
Leydecker House	Single residence	1.1	660
Leydecker Road	Bridge	1.2	666 (low steel)
Winspear Subdivision	Several residences	1.8–2.0	672
Brady's House	Single residence	2.1	676
Upstream House	Single residence	2.2	676

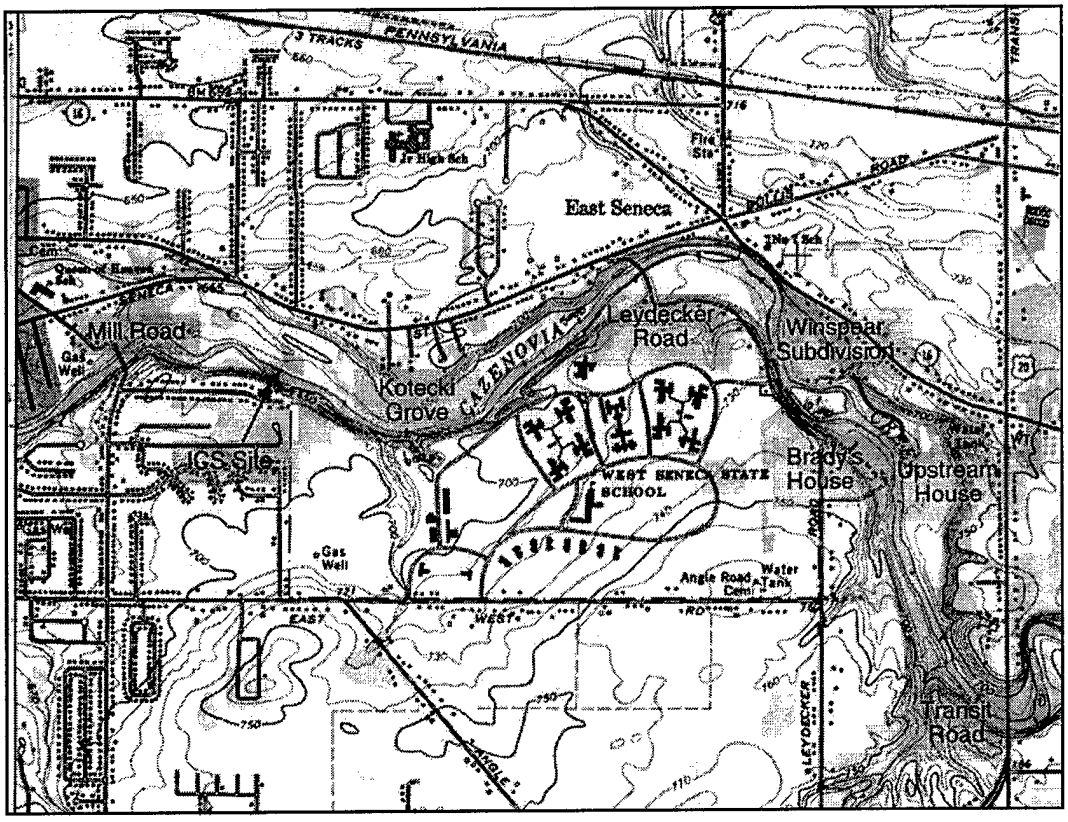

Figure 15. Topographic map of reach of Cazenovia Creek valley modeled for upstream effects caused by the cylindrical-pier ICS. (From USGS Orchard Park Quadrangle, 1965.)

volume upstream of the ICS. Nevertheless, we would expect the ICS to retain thick, strong ice well beyond the 6000-cfs design discharge.

The ICS jam will be grounded near the structure and free-floating beyond about 200 ft upstream. Beyond the grounded section, the ICS jam is hydraulically similar to a natural jam, adding a thick, rough, floating ice cover to the river. The jam produces much higher water levels along its length than would occur for the same discharge during open-water events. However, washouts and melting of smaller floes will reduce the retained ice volume (and hence reduce jam length) throughout the event. Beyond about 8000–10,000 cfs, the washout rate should accelerate, depending on the ice thickness and strength.

Ice jam volume

The volume of ice in the jam retained by the ICS governs the extent of high water induced upstream. This ice volume will change during a breakup event, and we require an estimate of the volume retained as a function of discharge, $V_j(Q)$. The initial ice run from upstream will leave ice floes along the banks (in the form of shear walls) and on the small floodplains that line the valley floor. Once the ICS forms a jam, melting and slow washouts will reduce its volume throughout the event. At high discharge, ice washouts will accelerate as floes break and release through the ICS gaps. We require estimates of each term in this process to determine $V_j(Q)$.

River ice supply

Buffalo District personnel conducted ice-thickness measurements in 1983 and aerial surveys in 1983 and 1985 to observe the ice-formation process and determine the ice supply in Cazenovia Creek (U.S. Army 1986b). They estimated that the pre-breakup ice supply "from the headwaters to Cazenovia Street" was 7.8 $\times 10^6$ ft^3 in 1983 and 9.2 $\times 10^6$ ft^3 in 1985. Although the ice-thickness data themselves are not available, maps used for the surveys during 1983 record about 0.7-ft-thick solid ice. Consequently, the thickness of solid ice in 1985 was probably about 0.9 ft. These volume estimates are consistent with ice covering 100% of the 16 miles of river from Cazenovia Street to East Aurora, assuming an average cover width of 120 ft.

The river length from the ICS site to East Aurora is about 11 miles. Along this reach, the average cover width should be about 100 ft. A good estimate of the maximum average ice thickness immediately prior to breakup is 1.5 ft. This yields an ice volume of 9×10^6 ft^3, which we may increase to 10×10^6 ft^3 to allow for minor ice supply from the east and west branches (U.S. Army 1986b). This becomes our best estimate for the pre-breakup ice supply, V_r.

Transport losses

Field measurements have shown that the ice volume in a breakup jam can be substantially less than the volume of the pre-breakup ice cover on the contributing river reach. The formation of shear walls and the stranding of ice floes on small floodplains are the main transport losses occurring during an ice run. The transport loss coefficient, C_t, is defined as the ratio of ice volume lost during a breakup run to the volume of the pre-breakup ice cover. It is thought to increase with the length of contributing reach (U.S. Army 1982).

Table 4 lists values of the C_t available in the literature and those calculated here for the 1972 and 1985 ice jams on Cazenovia Creek. We derived the latter values using reported jam locations and lengths (U.S. Army 1972, Predmore 1985). The transport loss coefficient is related to the ice-supply and ice-jam parameters as follows:

$$C_t = 1 - \frac{L_j}{L_r} \cdot \frac{B_j}{B_r} \cdot \frac{h_j}{y_i}(1-p) \qquad (3)$$

where L = length of the jam
B = width of the jam
h_j = thickness of the jam
p = porosity of the jam, assumed to be 0.4 (Prowse 1990)
L_r = length of the contributing ice cover
B_r = width of the contributing ice cover
t_i = average ice thickness of the contributing ice cover.

For ice jams on smaller rivers, typical values of $L_j/L_r \sim 0.1$, $B_j/B_r \sim 2$, $h_j/t_i \sim 4$ result in $C_t \sim 0.5$.

Nearly all of the available estimates of C_t, including ones based on jams in Cazenovia Creek, equal or exceed 0.3. The exception is for an ice jam on the Winooski River (which flooded Montpelier, Vermont, in March 1992), whose contributing reach was very short and had few overbank areas to strand ice. Therefore, although an average value of 0.5 could be justified, we will use $C_t = 0.3$ as a conservative estimate for transport losses.

Ice melting

Ice breakup normally occurs as a result of rapid snowmelt or rainfall during periods of above-freezing air temperatures. Upstream of an ice jam, air–water convection, solar radiation, groundwater inflow, fluid friction, and geothermal flux will all add heat to the river. Under the assumption that little ice remains upstream or that it has been stranded above the water level during the breakup surge, this heat flux will raise the temperature of water entering the head of the jam. The resulting melting (and weakening) of ice floes within a jam can be significant during long-duration, high-discharge events. Although loss of jam volume may not be visibly obvious, these effects probably couple with rising hydrodynamic forces to release natural ice jams.

Table 5 presents measurements of water temperature entering breakup ice jams. Because of the high flow velocities and ice-jam roughness, nearly all the available heat is transferred to ice melting within about 1 mile. If the jam is longer than this, ice melting at the upstream end will predominate. As the jam shortens, some warm water will persist to the toe and melt or weaken ice preferentially along main flow paths. In the case of a jam at an ICS, this process contributes to its ultimate release or washout.

The sensible heat of water is 1 Btu/lb$_m$ °F or about 62 Btu/ft^3 °F. The latent heat of fusion for ice is 144 Btu/lb$_m$ or about 8200 Btu/ft^3 for solid ice (specific gravity 0.92). Assuming 100% of the sensible heat of the

Table 4. Transport loss coefficients for breakup ice jams.

Reference	River	Contributing reach, L_r (mi.)	Transport loss coefficient C_t	Comments
Calkins (1978)	Ottaquechee R.	26	0.9	Assumed jam porosity of 0.4
		14	0.9	(Prowse 1986).
Prowse (1986)	Liard R.	300	0.8	Entire event.
		94	0.4	Last 24 hours of movement.
Cumming-Cockburn (1986)	Credit R.	9	0.5	3 years of field surveys.
Tuthill et al. (1996)	Winooski R.	3	0	Short reach, few overbank areas.
This work	Cazenovia Cr.	12	0.3–0.5	1972 ice jam.
		16	0.3–0.5	1985 ice jam.

Table 5. Measurements of water temperature entering breakup ice jams. The heat-transfer length is the distance from the head of a jam to the point where the water has lost > 90% of its sensible heat.

Reference	River	Entering water temp., ΔT (°F–32)	Heat-transfer length (miles)	Comments
Calkins (1984)	Ottaquechee R.	1.3	0.8	Upstream of refrozen jam, time between breakup and measurement unknown.
Prowse and Marsh (1989)	Liard R.	3.1	2	Measured during breakup event.
Beltaos et al. (1998)	Matapedia R.	4.5	0.2	Time between breakup and measurement unknown.
This work	Cazenovia Cr.	1.8	unknown	Measured by USGS about 12 hours after peak of 1985 ice-jam hydrograph.

water entering a jam is lost to melting ice, we relate the volumetric melt rate of ice, V_m, to discharge, Q, via:

$$\dot{V}_m \approx 0.008 \cdot Q(\text{cfs}) \cdot \Delta T(°\text{F}) \quad (4)$$

where ΔT is the water temperature difference above 32°F. Thus, water entering a jam 1°F above freezing will cause a volumetric melt rate of about 1% of river discharge. The data in Table 4 support a temperature difference at least this high. The expected rise in ΔT as the event proceeds should compensate for loss of sensible heat through the toe of the jam as it becomes shorter. Therefore, we will use $\dot{V}_m(\text{cfs}) = 0.01 \cdot Q(\text{cfs})$ as our best estimate for the volumetric melt rate of the ice jam retained by the ICS.

Ice washouts

During the model tests, we did not quantify the rate of ice loss attributable to major washouts or ultimate releases through the ICS. However, observations during washouts or releases at high discharge suggest approximately 1% ice concentrations downstream of the ICS. Washouts of smaller ice floes through the ICS and onto the floodplain also took place throughout the tests without release of the larger floes arched at the ICS. For simplicity, however, we will assume that the washout rate, $\dot{V}_w$, is zero below 8000 cfs, and increases to $\dot{V}_w(\text{cfs}) = 0.01 \cdot Q(\text{cfs})$ for discharge above 8000 cfs. By neglecting washouts at low discharge, this approach is probably conservative in its effect on ice jam volume.

Hydrograph rise time

To determine ice-jam volume lost up to a given discharge, we must integrate the loss rates (expressed in terms of river discharge) with respect to time. This requires an expression for the rise time of a characteristic hydrograph: the slower the rate of rise, the more ice volume is lost to melting and washouts up to a particular discharge.

We used the hydrographs from the 1972 and 1985 ice-jam events (see Fig. 2) to estimate the rise time for discharge after ice jam formation (i.e., from just after the initial spike to the broad, ice-free peak). This yielded 400 cfs/hr and 500 cfs/hr for the 1972 and 1985 events, respectively. We will use a straight-line hydrograph that rises at 500 cfs/hr from a jam-formation discharge of 2000 cfs. Although a hydrograph rises more slowly during the early portion of an event, use of the faster, near-peak rate produces a conservative estimate of the ice volume lost to melting and washouts.

Ice-jam volume versus discharge

We may combine the preceding terms to estimate the volume of ice in the jam retained by the ICS as a function of discharge, $V_j(Q)$. Transport losses of 30% reduce the estimated 10×10^6 ft^3 pre-breakup ice supply to an initial jam volume of V_j (2000 cfs) = 7×10^6 ft^3. Following a straight-line hydrograph that rises at 500 cfs/hr, melting losses occur at a rate of 1% of discharge throughout the event. Above 8000 cfs, additional losses ascribable to washouts at the ICS occur at a rate of 1% of discharge.

Figure 16 shows the resulting ice-jam volume at the ICS as a function of river discharge. Because losses increase with increasing discharge, ice jam volume decreases. Ice losses become particularly significant above about 8000 cfs, as we would expect from the model tests, and that just above 11,000 cfs we would expect essentially all the ice to have melted or washed out through the ICS. This estimate of $V_j(Q)$ should be conservative, and we used it to constrain the ice-jam length to predict upstream water levels.

Numerical ice–hydraulic model

Model formulation

We used HEC-RAS, the Corps' numerical hydraulic model (U.S. Army 1998a), to calculate water surface profiles through the ICS reach for both open-water and ice-jam cases. Briefly, HEC-RAS treats water flow

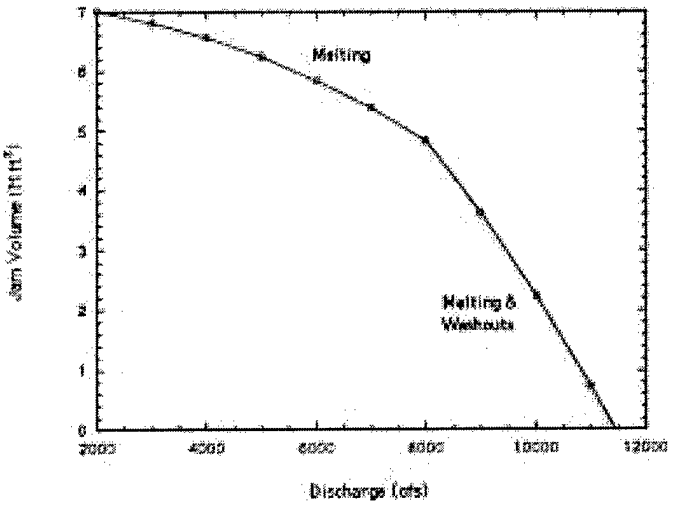

Figure 16. Volume of ice in the jam retained by the cylindrical-pier ICS as a function of river discharge. Transport losses reduce 10,000,000 ft^3 pre-breakup ice supply to an initial jam volume of 7,000,000 ft^3 at 2000 cfs. Ice melting, plus washouts through the ICS above 8000 cfs, reduce ice-jam volume as discharge increases throughout an event.

as one-dimensional, steady, and gradually varied (spatially), as did its predecessor HEC-2. At each cross section, it can include an ice cover of known thickness or solve for the thickness of an ice jam according to standard theory (U.S. Army 1998b). The latter is a steady-state theory that treats the ice as a granular material with no cohesion. The program solves the one-dimensional force balance for the jam, where the under-ice water shear and jam self-weight are resisted by the shear strength of ice at the banks. The ice jam floats on the water and adds a rough top surface, resulting in water levels that are much higher than for open water at the same discharge. The user can constrain the jam to the main channel (appropriate for treed floodplains) and can set hydraulic roughness (Manning's n) of the ice to a fixed value or allow it to vary with jam thickness. The program calculates the volume of ice in a jam, allowing us to simulate a jam of known volume at each discharge (upstream of which is open water).

Input to the numerical model included 50 cross sections along 3.6 miles of Cazenovia Creek, from 600 ft downstream of Mill Road to 100 ft downstream of Transit Road (see Fig. 15). The cross sections came from three sources: 1) an HEC-2 deck called Cazpfe that used surveyed cross sections from 1984, 2) closely spaced surveyed cross sections obtained in 1998 to construct the physical model, and 3) supplemental cross sections determined from topographic maps (1 in. = 200 ft) obtained from the Town of West Seneca. As far as possible, we checked these data for consistency in terms of vertical and horizontal alignment. The HEC-2 deck included the geometry of the two bridges in the reach, at Mill Road and Leydecker Road. We input the 5-ft-diameter ×10-ft-tall × 12-ft-gap cylindrical-pier ICS using the HEC-RAS feature "multiple blocked obstructions."

All model runs used subcritical flow. The downstream rating curve derived from the output of the HEC-2 deck (RS 308.00, U.S. Army 1986b). Several calibration flows were used to compare computed water-surface elevations (WSE's) with physical-model and field data. Final runs were made using the 100-year (1%-exceedence) open-water flow of 15,600 cfs and ice-jam flows of 4000–13,000 cfs.

Model calibration

Open-water WSE data without the ICS were available from three sources: 1) field measurements along the ICS site in 1984 at discharges of 783 and 3170 cfs, 2) a HEC-2 computed water-surface profile at 2000 cfs (U.S. Army 1986b), and 3) a water-surface profile at 15,600 cfs from a recent flood insurance study (FEMA 1992). As shown in Figure 17, minor adjustment of channel and over-bank roughness values along the reach gave good agreement between the calibration data and the HEC-RAS model results at these four discharges.

Open-water WSE data with the ICS were available from the physical model at discharges of 1550, 2900, and 5800 cfs. We used these to adjust the contraction and expansion coefficients in the HEC-RAS model to calibrate the water-level change across the ICS (Fig. 18).

No WSE field data were available for ice-jam conditions upstream of Mill Road, probably because this

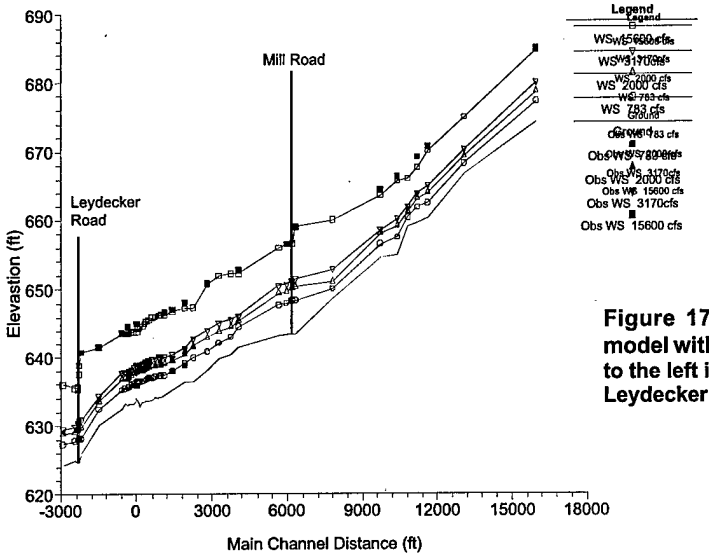

Figure 17. Open-water calibration of HEC-RAS model without ICS (Plan 61). The vertical line farthest to the left is the location of Mill Road, and the other is Leydecker Road.

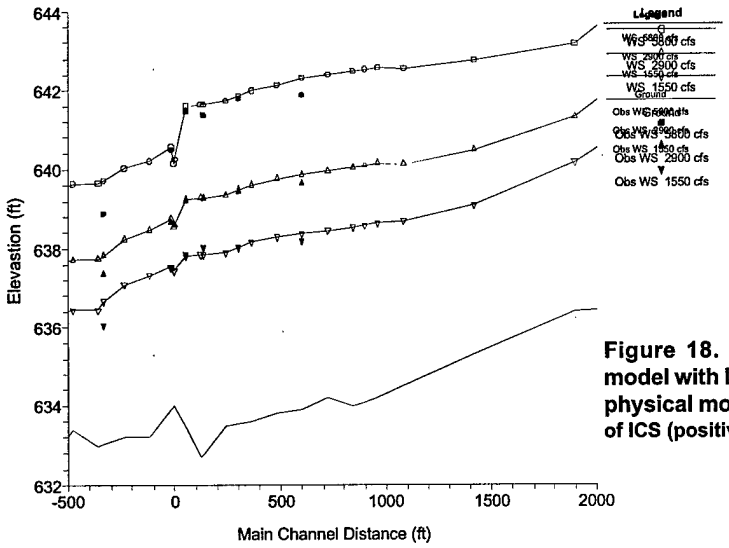

Figure 18. Open-water calibration of HEC-RAS model with ICS (Plan 60). Observed WSE's are from physical model. Channel distance is relative to location of ICS (positive upstream).

has not been an area of concern during past events. The ice run through the reach in 1985 caused 5- to 6-ft-high shear walls upstream of both Mill Road and Leydecker Road (Predmore 1985), although these probably reflect very dynamic jam formation and collapse processes at the onset of the event (say, 2000–4000 cfs). Also, local residents (J. Durand and J. Brady) noted that ice runs have caused below-flood-stage elevations at and upstream of Winspear Road, but they differed in opinion about whether stationary jams formed.

The physical model provided WSE data with the ICS for many different ice-jam conditions. We selected three data sets (2000, 6000, and 6100 cfs) that offered fairly long, steady-state ice jams upstream of the ICS. As with all the tests, however, the jams were grounded at the ICS, a feature that cannot be modeled directly with HEC-RAS. Instead, we matched the measured WSE's by setting 6-ft-thick ice covers along the first 50 ft upstream of the ICS (Fig. 19). We selected a conservative value of 0.08 for Manning's n of the underside of the ice jam and used this for all the final ice-jam runs. Runs conducted with variable Manning's n (i.e., n dependent on jam thickness) yielded similar results. Also, runs with the ice jam toe at Mill Road converged with these results about 1000 ft upstream of the ICS, indicating that river geometry governs ice-jam thickness except near the structure. At ice-jam discharges of 9000–12,000 cfs, we thickened the jam toe to 8 ft and

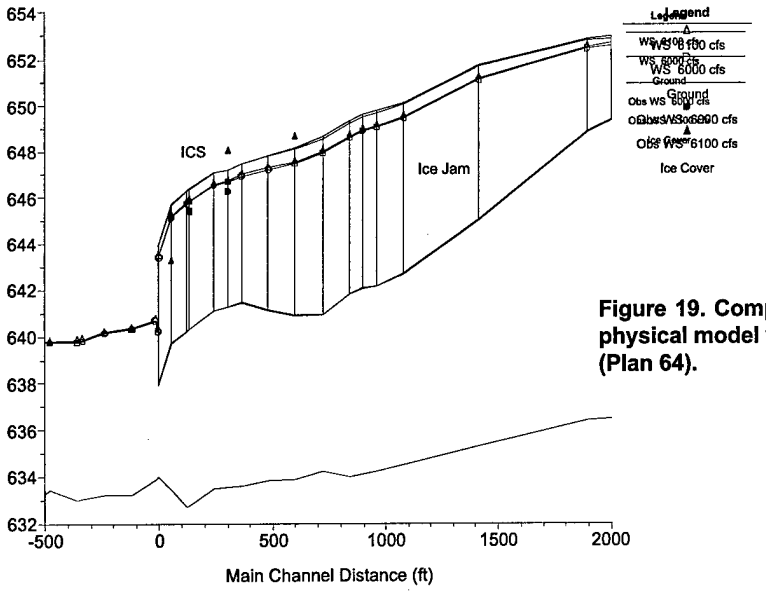

Figure 19. Comparison of WSE's measured in the physical model with HEC-RAS results near the ICS (Plan 64).

extended it to 300 ft upstream of the ICS to achieve stable calculations near the ICS.

Results

Figure 20 shows the open-water profiles for the 100-year discharge (15,600 cfs) with and without the ICS. The effect of the ICS disappears beyond about 2500 ft upstream. Although the ICS raises the 100-year open-water flood elevation at Kotecki Grove by about 0.6 ft, ice jam conditions actually dictate maximum WSE at this location.

Figure 21 shows ice-jam profiles at 4000, 7000, and 10,000 cfs, with ice volume limited according to discharge (see Fig. 16). HEC-RAS requires a fixed ice-jam thickness at the head of a jam, and we used 1.5 ft (i.e., the parent ice cover thickness) for all calculations. Open-water conditions prevail upstream of a jam. Figure 21 shows that jam length decreases dramatically with increasing discharge, a combination of decreasing ice volume and increasing jam thickness.

We determined the maximum water levels expected upstream of the ICS by assembling the open-water and ice-jam profiles for all discharges into a single data file. Figure 22 shows typical results. Where the profiles cross, the discharge that establishes the maximum WSE changes. Table 6 provides the maximum WSE, the dis-

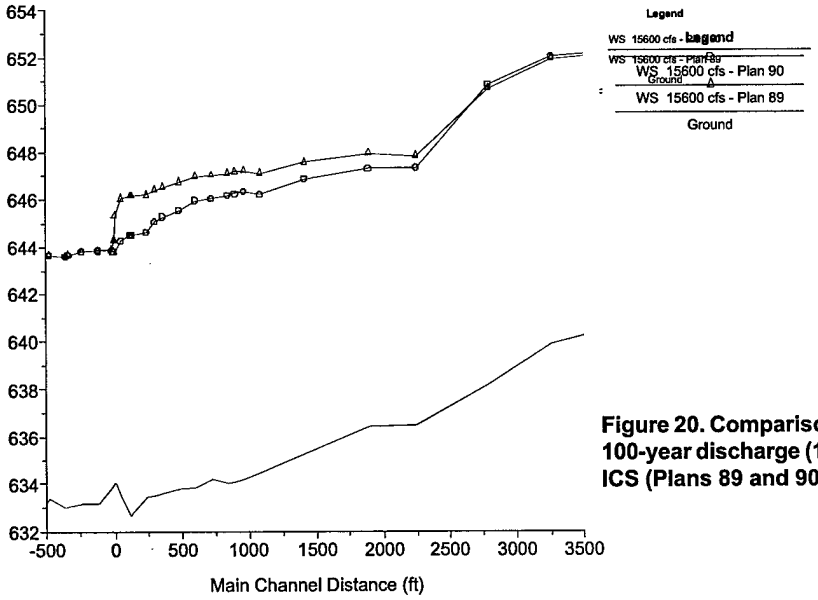

Figure 20. Comparison of open-water profiles at the 100-year discharge (15,600 cfs) with and without the ICS (Plans 89 and 90, respectively).

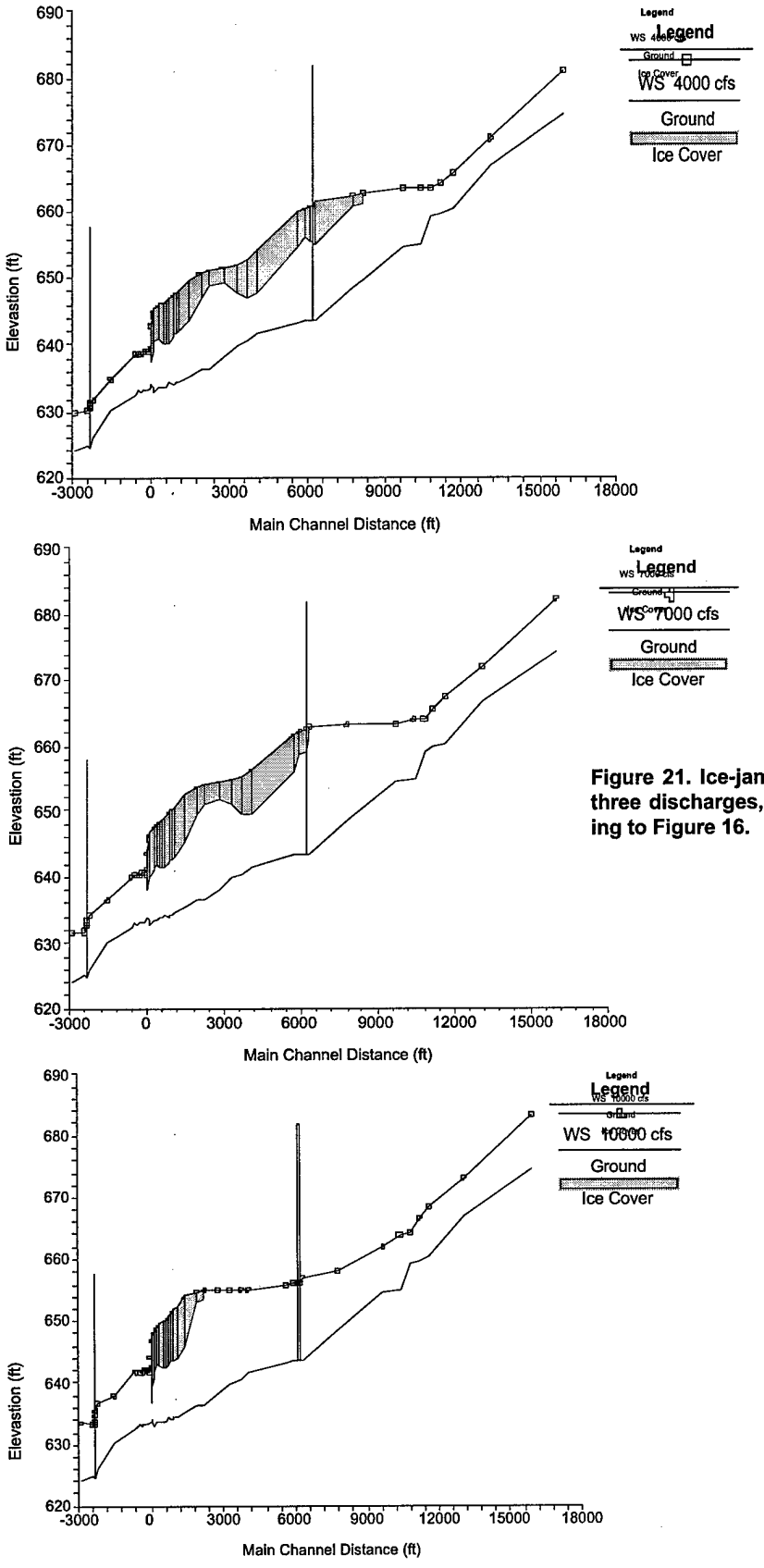

Figure 21. Ice-jam profiles induced by the ICS at three discharges, with ice volume limited according to Figure 16.

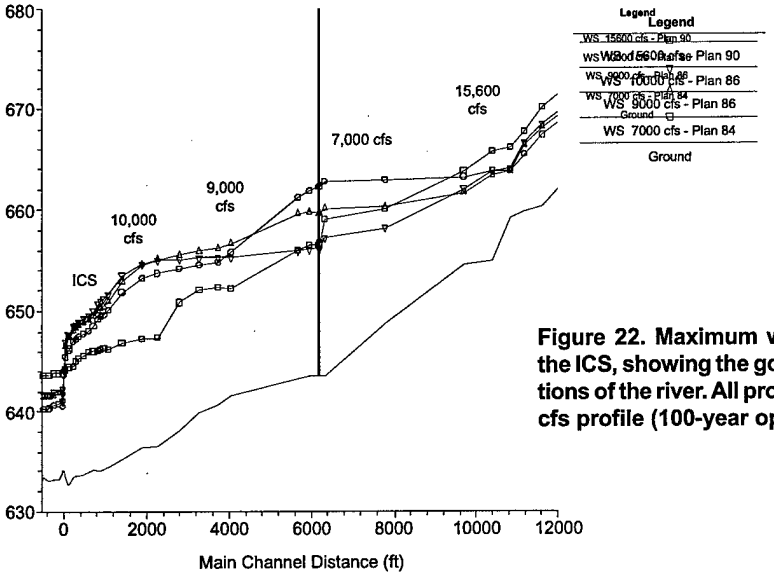

Figure 22. Maximum waterlevels expected upstream of the ICS, showing the governing discharge for various sections of the river. All profiles are for ice jams except 15,600-cfs profile (100-year open water).

Table 6. Maximum waterlevels expected upstream of the ICS. Note that the ICS has no effect beyond about 9600 ft upstream, where the 100-year open-water profile dictates maximum waterlevels. The ICS is located at the site originally proposed for the weir-with-pier ICS (USACE 1986a, 1986b), identified as RS 337.27 in Cazpfe HEC-2 deck.

Distance upstream of ICS (ft)	*Maximum water surface elevation (ft-NGVD)*	*Governing discharge (cfs)*	*Open water or ice conditions*	*Landmark*
15962	684.74	15600	Open-Water	
13062	674.93	15600	Open-Water	
11618	670.10	15600	Open-Water	Upstream House
11178	667.62	15600	Open-Water	Brady's House
10818	666.15	15600	Open-Water	
10403	665.79	15600	Open-Water	Winspear Subdivision
9692	663.72	15600	Open-Water	Winspear Subdivision
7792	662.98	7000	Ice	
6292	662.71	7000	Ice	
6192	662.31	7000	Ice	Leydecker Rd
6164	662.23	7000	Ice	Leydecker Rd
5950	661.86	7000	Ice	Leydecker House
5650	661.23	7000	Ice	
4037	656.64	9000	Ice	
3727	656.13	9000	Ice	
3252	655.86	9000	Ice	
2782	655.52	9000	Ice	
2247	655.00	9000	Ice	
1892	654.58	10000	Ice	Kotecki Grove
1417	653.52	10000	Ice	Kotecki Grove
1080	651.66	10000	Ice	
960	651.15	10000	Ice	
897	650.98	10000	Ice	
840	650.69	10000	Ice	
720	650.02	10000	Ice	
600	649.73	11000	Ice	
480	649.50	11000	Ice	
360	649.29	11000	Ice	
299	648.96	11000	Ice	
240	648.84	11000	Ice	
132	648.10	11000	Ice	
120	647.98	11000	Ice	
50	647.13	11000	Ice	
0	645.34	15600	Open-Water	ICS

charge that establishes that WSE, and governing surface condition (open-water or ice-jam) at each cross section.

At the Winspear Subdivision and above, the 100-year open-water profile dictates maximum water levels. That is, the ICS has no effect on water levels beyond about 9600 ft upstream. From there to below the Leydecker House, the 7000-cfs ice-jam profile dictates maximum water levels. The governing ice-jam discharge then increases with proximity to the ICS, such that 10,000 cfs dictates the maximum water level expected at Kotecki Grove. Of the structures within the Cazenovia Creek valley (Table 3), only Kotecki Grove and the Leydecker House are affected by ice jams at the ICS. Note also that ice jams at the ICS do not contact the bridge at Leydecker Road (low-steel elevation 666.00 ft).

DISCUSSION

The cylindrical-pier ICS is a refinement of the sloped-block ICS installed in Hardwick, Vermont. These wide-gap structures arrest breakup ice runs, retain the partially grounded ice jams, and use existing treed floodplains to bypass flow. They function well without requiring a weir or prepared floodway. Cylindrical piers with 12-ft gaps should retain ice, particularly thin ice, at much higher discharge than sloped blocks with 14-ft gaps. For breakup events that pose the greatest flood threat (thick, strong ice, heavy rain, or rapid snowmelt), the cylindrical-pier ICS should retain ice until well after ice has cleared from downstream reaches. Thus, this new ICS should substantially reduce ice-jam flood damages along Cazenovia Creek in West Seneca.

Construction plans, specifications, and cost estimates were completed for the original weir-with-piers ICS (US Army 1986a). The most expensive items were common excavation, compacted fill, and concrete with forming (for the upstream pool, prepared floodway, and weir-with-piers structure, respectively). The new ICS eliminates the first two items and substantially reduces the third. We may estimate approximately 50% cost savings for the remaining items (e.g., clearing and grubbing, roadways, riprap, engineering, supervision, land). The construction cost for the new ICS might thus be about one-quarter to one-third of the cost of the original ICS. The new ICS will not have a gate to operate and will not require dredging to remove deposited sediment. Despite these lower costs, model results suggest that it should perform at least as well as the original concept.

The calibrated HEC-RAS model should provide reliable estimates of the water-surface profiles expected for both open-water and ice-jam events, with and without the ICS. Because ice-jam water levels are so much higher than even 100-year open-water ones, the jam length or volume essentially governs the upstream influence of the structure. Insofar as possible, we have based the terms that affect jam volume on data from the physical model, the literature, or ice-jam events in Cazenovia Creek itself, and have selected values at the conservative end of the ranges for each term. Consequently, the predicted maximum water levels caused by the ICS should be conservative.

CONCLUSIONS

We recommend, as the new Cazenovia Creek ICS, a structure consisting of nine 5-ft-diameter × 10-ft-tall cylindrical piers spaced with 12-ft-gaps across the main channel. The treed floodplain should be left intact to act as a flow-bypass channel. About 300 ft of riprap is needed along the right bank near the structure to prevent scour and to delay reentry of floodplain flow until farther downstream. Comparison of the model results indicates that the new ICS should have an ice-retention capability at least as high as the original weir-with-piers ICS. For ice thickness approximately 1 ft or greater, we would expect the ICS to arrest a breakup ice run and retain the ice jam for a discharge exceeding 7000 cfs. Slow washouts, rather than catastrophic releases, will likely be the release mode at higher discharges or with thinner ice. We saw no performance advantage for a cylindrical-pier ICS with 10-ft gaps, whereas one with 14-ft gaps allowed ice washouts more easily. Because the new ICS does not include a weir and excavated pool, and makes use of the existing floodplain as a bypass channel, it should be substantially cheaper than the original weir-with-piers ICS.

Interestingly, the analysis for upstream effects has revealed the ice-retaining capacity of the ICS as a balance between two needs: the need to protect downstream areas from natural ice-jam flooding with the need to minimize upstream flooding by jams at the ICS. Melting and slow washout of ice through the ICS reduces extent of flooding upstream without endangering flooding downstream. Within our present capabilities for physical and numerical modeling, the 12-ft-gap, cylindrical-pier ICS appears to strike a good balance of these competing needs.

LITERATURE CITED

AASHTO (1998) *LRFD Bridge Design Specifications.* American Association of State Highway and Transportation Officials, Washington, D.C., Section 3.9.

Beltaos, S., J.S. Ford, M. Pedrosa, N.K. Madsen, and B.C. Burrell (1998) Remote measurements of temperature and surge levels in ice-laden rivers. In *Ice in Sur-*

face Waters (H.T. Shen. Ed.), *Proceedings of 14th International Symposium on Ice, Potsdam, New York*, vol. 1, pp. 34–40.

Calkins, D.J. (1978) Physical measurements of river ice jams. *Water Resources Research*, **14**(4): 693–695.

Calkins, D.J. (1984) Ice cover melting in a shallow river. *Canadian Journal of Civil Engineering*, **17**: 255–265.

CRC (1970) *Handbook of Tables for Applied Engineering Science* (R.E. Bolz and G.L. Tuve, Ed.). Cleveland, Ohio: CRC Press, Chemical Rubber Co.

CSA (1988) *Design of Highway Bridges*. Canadian Standards Association, Rexdale, Ontario, CAN/CSA-S6-88.

Cumming-Cockburn & Associates (1986) Mississauga Ice Control Project. Credit Valley Conservation Authority, Meadowvale, Ontario.

Deck, D. (1984) Controlling river ice to alleviate ice jam flooding. In *Proceedings, IAHR Ice Symposium, Hamburg, Germany*. International Association for Hydraulic Research, vol. III, pp. 69–76.

Federal Emergency Management Agency (1992) Flood insurance study, Town of West Seneca, New York, Erie County. FEMA, Washington, D.C.

Gooch, G.E., and D.S. Deck (1990) Model study of the Cazenovia Creek ice control structure. U.S. Army Cold Regions Research and Engineering Laboratory, Special Report 90-29.

Hopkins, M.A., S.F. Daly, and J.H. Lever (1996) Three-dimensional simulation of river ice jams. In *Proceedings, Eighth International Conference on Cold Regions Engineering, ASCE, Fairbanks, Alaska*. American Society of Civil Engineers, pp. 582–593.

Lever, J.H., and G. Gooch (1998) Model and field performance of a sloped block ice control structure. In *Ice in Surface Waters* (H.T. Shen, Ed.), *Proceedings of 14th International Symposium on Ice, Potsdam, New York*, vol. 2, pp. 647–652.

Lever, J.H., G. Gooch, A. Tuthill, and C. Clark (1997) Low-cost ice-control structure. *Journal of Cold Regions Engineering, ASCE*, **11**(3): 198–220.

Montgomery, C.J., and A.W. Lipsett (1980) Dynamic tests and analysis of a massive pier subjected to ice forces. *Canadian Journal of Civil Engineering*, **7**: 432–441.

Montgomery, C.J., R. Gerard, and A.W. Lipsett (1980) Dynamic response of bridge piers to ice forces. *Canadian Journal of Civil Engineering*, **7**: 345–356.

Montgomery, C.J., R. Gerard, W.J. Huiskamp, and R.W. Kornelsen (1984) Application of ice engineering to bridge design standards. *Proceedings, Cold Regions Engineering Specialty Conference, Canadian Society for Civil Engineering, Montreal, Quebec*, vol. II, pp. 795–811.

Predmore, S.R. (1985) Field trip report Cazenovia Creek 23 February 1985. Notes on file at U.S. Army Engineer District, Buffalo, New York (unpublished).

Prowse, T.D (1986) Ice jam characteristics, Liard-Mackenzie rivers confluence. *Canadian Journal of Civil Engineering*, **13**: 653–665.

Prowse, T.D. (1990) Heat and mass balance of an ablating ice jam. *Canadian Journal of Civil Engineering*, **17**: 629–635.

Prowse, T.D., and P. Marsh (1989) Thermal budget of river ice covers during breakup. *Canadian Journal of Civil Engineering*, **16**: 62–71.

Tuthill, A.M., J.L. Wuebben, S.F. Daly, and K.D. White (1996) Probability distributions for peak stage on rivers affected by ice jams. *Journal of Cold Regions Engineering*, **10**(1): 36–57.

U.S. Army Corps of Engineers (1972) Report of the flood of 1–7 March 1972 Western New York in Buffalo District. U.S. Army Engineer District, Buffalo, New York.

U.S. Army Corps of Engineers (1975) Interim report on feasibility of flood management in Cazenovia Creek Watershed. Technical appendix. U.S. Army Engineer District, Buffalo, New York.

U.S. Army Corps of Engineers (1982) Ice engineering. Engineer Manual EM 1110-2-1621, Office of the Chief of Engineers, Washington, D.C., Chapter 8, pp. 5–7.

U.S. Army Corps of Engineers (1986a) Cazenovia Creek, West Seneca, New York, detailed project report and environmental impact statement, main report—final. U.S. Army Engineer District, Buffalo, New York.

U.S. Army Corps of Engineers (1986b) Cazenovia Creek, West Seneca, New York, final detailed project report, appendices—final. U.S. Army Engineer District, Buffalo, New York.

U.S. Army Corps of Engineers (1998a) HEC-RAS river analysis system, user's manual, version 2.2. Hydrologic Engineering Center, Davis, California.

U.S. Army Corps of Engineers (1998b) HEC-RAS river analysis system, hydraulic reference manual, version 2.2. Hydrologic Engineering Center, Davis, California, Chapter 11, pp. 1–8.

REPORT DOCUMENTATION PAGE

Form Approved
OMB No. 0704-0188

1. REPORT DATE *(DD-MM-YY)*	2. REPORT TYPE	3. DATES COVERED *(From - To)*
August 2000	Technical Report	

4. TITLE AND SUBTITLE

Cazenovia Creek Ice-Control Structure

5a. CONTRACT NUMBER

5b. GRANT NUMBER

5c. PROGRAM ELEMENT NUMBER

6. AUTHOR(S)

James H. Lever, Gordon Gooch, and Steven F. Daly

5d. PROJECT NUMBER

5e. TASK NUMBER

5f. WORK UNIT NUMBER

7. PERFORMING ORGANIZATION NAME(S) AND ADDRESS(ES)

U.S. Army Engineer Research and Development Center
Cold Regions Research and Engineering Laboratory
72 Lyme Road
Hanover, New Hampshire 03755-1290

8. PERFORMING ORGANIZATION REPORT NUMBER

ERDC/CRREL TR-00-14

9. SPONSORING/MONITORING AGENCY NAME(S) AND ADDRESS(ES)

U.S. Army Engineer District, Buffalo
1776 Niagara Street
Buffalo, New York 14207

10. SPONSOR / MONITOR'S ACRONYM(S)

11. SPONSOR / MONITOR'S REPORT NUMBER(S)

12. DISTRIBUTION / AVAILABILITY STATEMENT

Approved for public release; distribution is unlimited.

Available from NTIS, Springfield, Virginia 22161.

13. SUPPLEMENTARY NOTES

14. ABSTRACT

Cazenovia Creek, in Western New York, is the largest tributary of the Buffalo River. Breakup ice jams form along the lower basin nearly every year during mid-winter or spring thaws, and ice-jam flooding occurs in the City of Buffalo and the Town of West Seneca about every 2–3 years. This report describes physical model tests and design recommendations for a new ice-control structure (ICS) for Cazenovia Creek. The recommended structure consists of nine 10-ft-tall × 5-ft-diameter cylindrical piers spaced across the main channel, and it uses the adjoining treed floodplain as a natural bypass channel. Also described are results from a numerical ice–hydraulic model to determine the extent of flooding induced upstream of the new ICS. Although few structures are affected, the ice jam held by the ICS will cause minor flooding of properties abutting the creek. However, the stream-wise extent of this flooding will decrease during an event as melting and washouts reduce the volume of ice in the jam. The structure balances the need to protect downstream areas from natural ice-jam flooding and the need to minimize upstream flooding induced by the retained ice.

15. SUBJECT TERMS

Buffalo River
Cazenovia Creek
Ice
Ice control
Ice jams

16. SECURITY CLASSIFICATION OF:			17. LIMITATION OF ABSTRACT	18. NUMBER OF PAGES	19a. NAME OF RESPONSIBLE PERSON
a. REPORT	b. ABSTRACT	c. THIS PAGE			19b. TELEPHONE NUMBER *(include area code)*
U	U	U	U	27	